Transforming CO_2 into Formic Acid: An Eco-Efficient Design in Italy

Nikolaos Kalmoukidis*,[1], Maximiliano Taube*, Savvas Staikos*, Amsalia Barus*
* Delft University of Technology
Scientific & Design Supervisors: **Anton A. Kiss, Farzad Mousazadeh**

ABSTRACT
This study introduces a novel and eco-efficient CO_2 hydrogenation process design. Following an extensive literature review, Formic Acid (FA) emerged as a viable bulk chemical. A market analysis was performed to estimate feedstock availability. The plant, located in Ravenna, Italy, can produce 50 kta of 85 %wt. FA. The conversion of CO_2 and green H_2 into FA was meticulously analyzed to identify the best operating conditions and separation technologies, including COPure^{TM}. A key innovation of the sustainable process, simulated in Aspen Plus, is the implementation of Dividing Wall Column (DWC) configuration, which along with heat integration, results in 64% electricity savings, 20% less stream requirements and 51% reduction in CO_2 emissions compared to conventional processes. A 2030 economic assessment estimates capital investment and production costs at 73.8 M€ and 41.8 M€/yr respectively, with a profit of 9.5 M€/yr. A sensitivity analysis showed that profitability is heavily impacted by natural gas and product prices. Future carbon taxation and energy or cost-saving initiatives could further increase profitability, making this process a compelling alternative to current methods.

KEYWORDS Carbon dioxide; green Hydrogen, Formic Acid, Computer-aided Process Engineering

Introduction
The current effects of climate change, caused by human activities, demand urgent action to mitigate greenhouse gas emissions. In recent years, the European Union (EU) has taken significant steps by implementing the Renewable Energy Directive (RED). Initially, the RED set a target of 32% for renewable energy sources by the year 2030. However, this goal has been recently revised and raised to a minimum of 42.5% [1]. This shift highlights the critical importance of transitioning towards a low-carbon economy through innovative and sustainable approaches. One such approach involves valorizing captured CO_2 as a carbon feedstock and renewable energy resources for manufacturing valuable chemical products.
Researchers have increasingly focused on synthesizing bulk chemicals from CO_2 and green H_2. However, using sustainable feedstocks in the industrial sector presents two major challenges: (a) Availability and cost: While inexpensive CO_2 is readily available from various sources [2], the availability of low-cost hydrogen remains limited. (b) Process Adaptation: Implementing sustainable feedstocks often requires significant modifications to existing process lineups, posing economic and operational challenges.
In our work, we conducted a thorough literature review to gather the necessary information about the CO_2 hydrogenation of bulk chemicals, followed by a market review and key performance indicators (KPIs) to evaluate their economic feasibility and resilience. Among these chemicals, Formic Acid (FA) emerged as the most suitable candidate for developing a novel and eco-efficient production process from CO_2.
FA is a versatile chemical widely used in the food, pharmaceuticals, leather, and textile industries and serves as a promising hydrogen carrier due to its liquidity and chemical stability in ambient conditions. Its global market in 2019 was approximately US$ 760 million and is projected to grow by 4.5% annually until 2035, underlining its importance in economy and society [3].
Currently, at an industrial scale, FA is produced indirectly via Methyl Formate (MF) hydrolysis, using Methanol as a co-reactant and Syngas generated from fossil fuels [4]. Eco-friendlier FA synthesis

Manuscript compiled: Monday 15th April 2024
[1]n.kalmoukidis@tudelft.nl

methods have been reported in literature including conceptual or small-scale design approaches that utilize feedstocks such as biomass [5] or green Hydrogen for direct CO_2 hydrogenation [6]. In practice, however, implementing these methods in large industrial plants remains challenging and economically unfeasible. Particularly, direct gas-phase CO_2 hydrogenation towards FA faces a thermodynamic barrier due to the endergonic nature of the reaction ($\Delta G°_{300K}$ = 32.9 kJ·mol^{-1}) [7].

The present work's objective is to develop a conceptual novel process design for synthesizing FA from CO_2 hydrogenation. Introducing MF as an intermediate compound improves the thermodynamics of the reaction ($\Delta G°_{300K}$ = -5.3 kJ·mol^{-1}), as practiced in conventional FA production plants [8]. Transitioning from fossil fuels to CO_2 and green H_2 introduces several complexities. One significant hurdle is the separation of CO and N_2, which is an inert in CO_2, as their similar molecular sizes hinder size-based separation, and their close boiling points discourage the use of cryogenic methods. Additionally, the energy-demanding downstream processing of FA warrants attention and mitigation.

To overcome these challenges, this work incorporates process intensification (PI) techniques, such as the Dividing-wall Column (DWC) configuration, implements heat integration, and fine-tunes reaction conditions to facilitate the sustainable production of FA from CO_2 and green H_2. Upon completion of the simulation and technical design phase, an economic assessment will determine the project's financial viability and highlight significant cost contributors. Additionally, the performance and sustainability of the process will be benchmarked against conventional state-of-the-art FA chemical plants to demonstrate the overall reduction in energy consumption and in carbon footprint.

Literature Review

Selection of chemical product

Initially, literature research identified bulk chemicals that could be synthesized from CO_2 and green H_2. A two-step CO_2 hydrogenation reaction path was explored, involving Ammonia and Hydrochloric Acid. A conversion map was created, depicted in **Figure 1**, where light green signifies the products resulting from direct CO_2 hydrogenation, and blue indicates the involvement of an additional reaction.

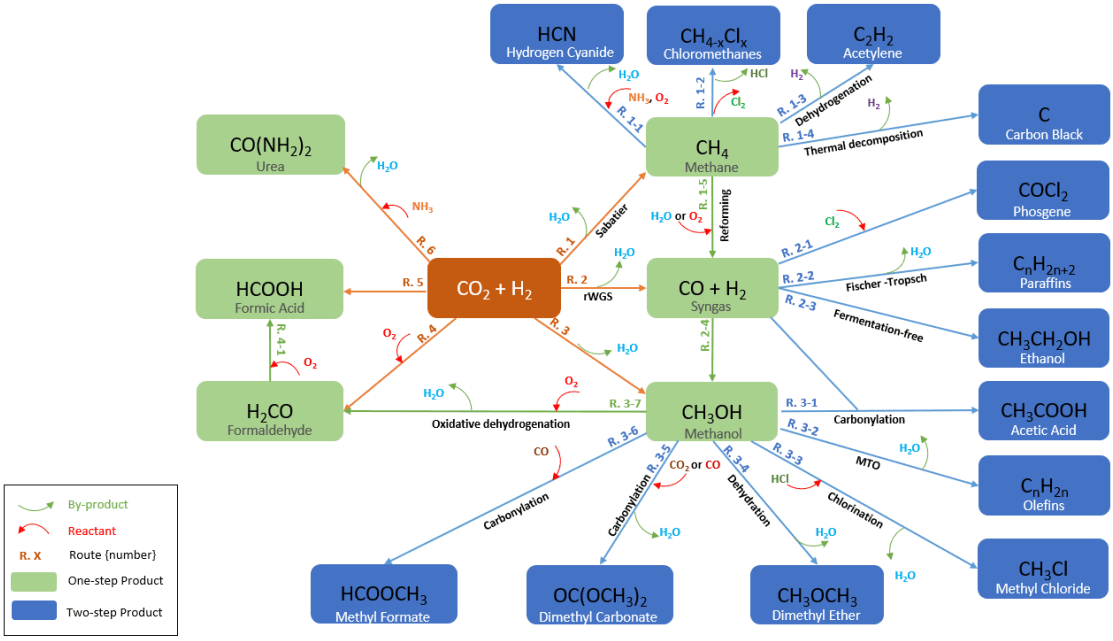

Figure 1: Diagram illustrating the conversion of CO_2 Hydrogenation into potential bulk chemicals

Several KPIs were chosen to facilitate an objective comparison and highlight the most viable routes for further exploration. An initial screening was carried out based solely on the Economic Margin. This was

computed using the following formula, considering the product price (*P*) and the cost of raw materials (*RM*) (CO_2 and H_2).

$$\text{Economic Margin} = P\left(\frac{€}{\text{ton}}\right) - RM\left(\frac{€}{\text{ton}}\right) \times \text{Quantity}\left(\frac{\text{ton } RM}{\text{ton } P}\right), \qquad [1]$$

In addition to the aforementioned factor, other KPIs that were considered, include the energy consumption (F_{eq}) per ton of product, the overall selectivity when using an optimal commercial catalyst, the enthalpy of the reaction and the available literature on kinetics to design this conceptual project. As illustrated in **Table 1**, FA emerges as the most viable final chemical product for this design project.

Table 1: Evaluation of various products that have positive margin

Route	Margin (€/ton)	F_{eq} consumption (GJ/ton)	Overall Selectivity (%)	ΔH_{300K} (kJ/mol)	Reason to reject
Syngas	302 [9]	21 [10]	99 [11]	-134	-
Methanol (direct)	85 [12]	8.3 [10]	82 [13]	-131	Low Margin
Methanol (indirect)	35 [12]	-	-	-	Low Margin
Formic Acid (direct)	574 [12]	11.9 [10]	99 [8]	-31	-
Formic Acid (indirect)	566 [12]	51.3 [14]	81 [15]	-146	-
Ethanol	252 [12]	87.2 [16]	71 [16]	-523	High F_{eq} to Margin ratio
Phosgene	1298 [17]	31.6 [18]	99 [19]	-241	Very Toxic
Acetic Acid	758 [12]	18 [20]	69 [21]	-400	Absence of novelty
Urea	86 [12]	5.6 [10]	99 [22]	-214	Low Margin
DME	236 [23]	5.7 [24]	82 [25]	-286	Absence of novelty
DMC	621 [12]	23.2 [26]	82 [27]	-696	Limited literature
Methyl Chloride	119 [23]	-	81 [28]	-258	Low Margin

Choosing the optimal FA synthesis route

Three potential routes for FA production were explored. Route 1 directly converts CO_2 and H_2 to FA via catalysis. Route 2 is an indirect method involving CO_2 hydrogenation to Methanol, which is then oxidized first to Formaldehyde (FD) and further to FA. Route 3, a commercial alternative, first converts CO_2 to CO, which reacts with Methanol to form MF via carbonylation, and finally hydrolyzes MF to FA. The direct synthesis route was deemed unfeasible due to high catalyst costs (ruthenium-phosphine), significant leaching from homogenous catalysis, and the need for amines and Methanol. The indirect route, based on industrially applicable Methanol oxidation to FD, was also rejected due to negative margins. The MF route, however, showed positive margins and was selected as the most promising (illustrated in **Figure 2**). This process involves the well-established carbonylation of Methanol to MF, followed by its hydrolysis to produce FA. Methanol is not consumed in this process but recycled.

Chemical reactions

CO is derived from the reverse Water Gas Shift (rWGS) reaction, utilizing CO_2 and green H_2 as feedstocks, as shown in equation (2).

$$CO_2 + H_2 \rightleftharpoons CO + H_2O, \qquad \Delta H_{300K} = 41.2\ \frac{\text{kJ}}{\text{mol}}, \qquad [2]$$

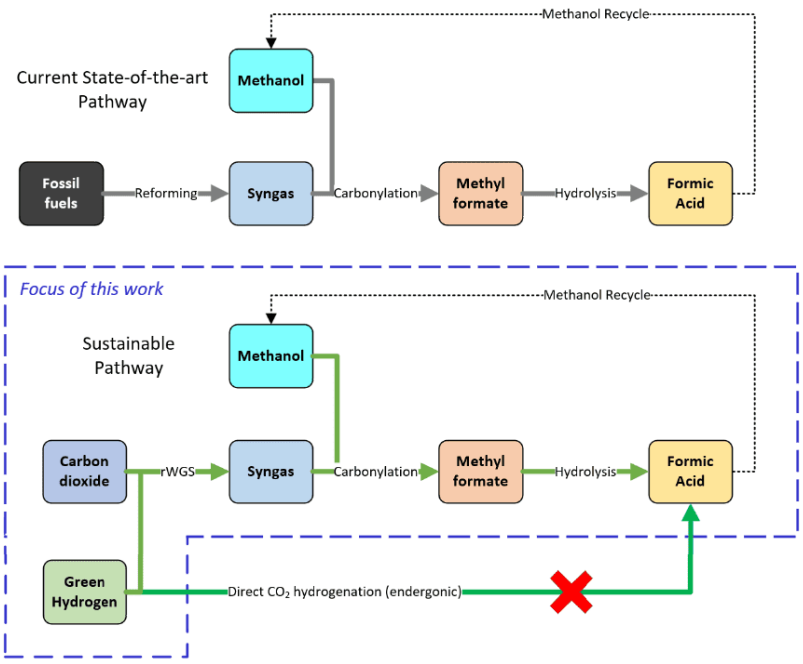

Figure 2: The approach of green FA production in this work.

To prevent the formation of Methane and Methanol during the rWGS reaction, it is necessary to maintain a H_2:CO_2 molar ratio below 3, high temperatures, and near-atmospheric pressure [29, 30]. Subsequently, CO undergoes carbonylation to produce MF, with Methanol as a co-reactant, as shown in equation (3).

$$CH_3OH + CO \rightleftharpoons HCOOCH_3, \qquad \Delta H_{300K} = -29.3\ \frac{kJ}{mol}, \qquad [3]$$

The carbonylation process, typically conducted in the liquid phase, benefits from high pressure as it enhances CO's solubility in Methanol, thereby improving the overall efficiency of the synthesis process [31]. The exothermic nature of the reaction favors equilibrium at lower temperatures, while the kinetics require higher temperatures, creating a trade-off. Research on MF synthesis is conducted under mild temperature conditions, typically between 60 and 110 °C [14]. An excess of methanol is essential to shift the equilibrium towards MF production. The CH_3OH:CO molar ratio ranges from 1 to 5, ensuring nearly complete conversion of CO while keeping Methanol conversion levels around 30% [32]. Excess Methanol is typically recovered through distillation and recycled back to the carbonylation reactor.

In the last step, MF hydrolysis yields FA, as illustrated in equation (4). While no side reactions occur, FA synthesis through this pathway is challenged by equilibrium constraints. A water-to-ester ratio between 0.8 and 7is recommended to balance FA production and energy costs [4]. The reaction, occurring in the liquid state, does not significantly depend on pressure but requires elevated pressure to maintain the volatile MF in the liquid phase ($T_{b,MF}$ = 31.8 °C at 1 atm). Higher temperatures favor FA synthesis [33], with an optimum at 120 °C due to FA's thermal decomposition to CO and H_2 [34]. The produced FA is then distilled to remove Methanol, excess water, and unreacted MF. Due to an azeotropic maximum between FA and water, distillation must be performed at 3 bar to achieve the target purity of 85 %wt. [4, 14]. Higher pressure is avoided to prevent up to 10% loss of FA due to thermal decomposition [35].

$$HCOOCH_3 + H_2O \rightleftharpoons CH_3OH + HCOOH, \qquad \Delta H_{300K} = 16.3\ \frac{kJ}{mol}, \qquad [4]$$

Catalysts and kinetics

Typical catalysts for the rWGS reaction include transition metals such as Iron, Cobalt, and Nickel, as well as metal oxides like Copper Oxide or Cerium Oxide [36]. Molybdenum Carbide (Mo_2C) has been reported

as one of options for its relatively cheap price and high activity in C=O bond scission and H_2 dissociation [37].The selected catalyst in this project is 1K-5Cu/β-Mo_2C, which was reported by Jingjing Xu et al. to deliver 100% CO selectivity and 48% one-pass CO_2 conversion (close to equilibrium) under operating conditions of 600 °C, 1 bar, and WHSV of 84000 mL/g/h [38].

For MF synthesis commercial Sodium Methoxide catalyst was chosen. The high purity of the previously produced CO is crucial, given the catalyst's susceptibility to residual water and CO_2 [32]. The kinetics that dictate MF synthesis under this catalyst were inferred from the study carried out by Bai et al. [14], which considers both the forward and backward reactions. In line with the parameters from the mentioned study, the catalyst concentration used for the process was 0.408 mol/$L_{reactor}$ of Sodium Methoxide (2.5 %wt.), with a residence time of 0.717 h. The MF carbonylation reaction kinetic is:

$$r_{MF} = 1.41 \times 10^{9} e^{-\left(\frac{70748}{RT}\right)} [cat]_L [\mathrm{CH_3OH}]_L [\mathrm{CO}]_L - \ 2.51 \times 10^{12} e^{-\left(\frac{92059}{RT}\right)} [cat]_L [\mathrm{HCOOCH_3}]_L, \qquad [5]$$

The hydrolysis of MF takes place in two reactors with distinct kinetic models [39]. Initially the hydrolysis is auto-catalysed, following the kinetics outlined below [40]:

$$r_{FA} = \bar{k} e^{-\left(\frac{E_a}{R}\left(\frac{1}{T}-\frac{1}{T_R}\right)\right)} \left\{1 + \frac{\bar{k'}}{\bar{k}} \, e^{-\left(\frac{E_a}{R}\left(\frac{E'_a}{E_a}-1\right)\left(\frac{1}{T}-\frac{1}{T_R}\right)\right)} C_C\right\} \left(C_A C_B - \frac{1}{K_C} C_C C_D\right), \qquad [6]$$

When a sufficient amount of FA is available, an excess of water is added to the reactor and the reaction proceeds with FA as the catalyst. The kinetic model in this case is [41]:

$$r'_{FA} = \bar{k'} \, (K_d C_C)^{0.5} e^{-\left(\frac{E'_a}{R}\left(\frac{1}{T}-\frac{1}{T_R}\right)\right)} \left(C_A C_B - \frac{1}{K_C} C_C C_D\right), \qquad [7]$$

Table 2 includes all the kinetic parameters that were considered for simulating the two chemical reactors in Aspen Plus V12 [14].

Table 2: Kinetic parameters for FA synthesis simulation

Kinetic model	k' [L^2 mol^{-2} s^{-1}]	E_a' [kJ mol^{-1}]	k [L^2 mol^{-2} s^{-1}]	E_a [kJ mol^{-1}]	K_c	K_d	Reference
Auto catalysed	0.002	66.4	4.33×10^{-4}	88.2	0.17	-	[40]
FA- catalysed	0.195	67.8	-	-	0.18	1.8×10^{-4}	[41, 42]

Process Capacity

In 2021, global FA production reached 710 kta and is expected to grow to 1000 kta by 2030 [43]. BASF is the leading FA manufacturer with plants operating across continents and total capacity of 305 kta [44]. Reported FA plant capacities range from 10 kta to 100 kta, with 50 kta serving as a mid-range size and representing the median. While the largest size benefits most from the economy of scale, a 100 kta project would be unique, as only BASF Germany currently operates at this capacity.

Our proposal aims to supply FA for consumption within Europe. According to a report by S&P, FA consumption in Europe accounted for 30-40% of global demand, which translates to 350 kta [45]. With the chosen capacity of 50 kta, production can satisfy 15% of the market demand, which is considered both sufficient and competitive.

Plant Location

The EU is emerging as a frontrunner in CO_2 utilization and green H_2 production, by introducing several regulations to encourage decarbonization, reflecting its determination and efforts to fulfill its commitment towards net zero emissions by 2050. These developments position Europe as an attractive host for green FA plants. A report from the European Commission reveals that Europe's current total FA plant capacity is approximately 350 kta. Germany houses 60% of this capacity, Finland 30%, and the remainder is distributed across the rest of the continent [8]. This implies that there will be an inevitable

competition with the major established FA entities. The selection of further locations was assessed by several crucial factors, including the availability of raw materials and utilities, market access, and transportation-logistic infrastructure. Among the potential sites, Ravenna in Northern Italy stands out for its strategic location. The Port of Ravenna, located on the North Adriatic Sea, is one of the key seaports in Italy and Europe. This advantageous location offers benefits, such as efficient supply chain management, seamless global market connectivity, and a well-developed infrastructure.

Feedstock availability

The availability of raw materials is a major criterion for location selection. Eni, an Italian oil and gas company, is in the process of developing one of the world's largest carbon storage hubs located in offshore Ravenna. The facility is projected to have a capacity of 16 Mta by 2030. The initial phase began in 2024 with the goal of capturing 25 kt of CO_2 from Eni's Casalborsetti gas processing plant. The capacity is expected to increase to 4000 kt of CO_2 by 2027 during the industrial phase, providing sufficient capacity to establish a stand-alone FA production plant [46].

Hydrogen is another key feedstock for FA production. Its availability and supply in Ravenna have also been evaluated. H_2 can be sourced either internally, where it is produced on-site, or externally, where it is obtained from the H_2 network. In the internal scenario, access to renewable energy is mandatory. So far, only solar and wind energy have been identified as renewable energy sources in Ravenna. A 6 MW solar PV facility is currently operational and is planned to be connected to the power grid this year [47]. Additionally, an offshore wind project with a capacity of 450 MW has been confirmed and is scheduled to be commissioned in 2026 [48]. Regarding the external scenario, the SouthH_2 corridor project serves as a potential H_2 source. This pipeline connects the north Africa region, a major producer of green H_2, with Italy, Austria, and Germany and is expected to be operational by 2030 [49]. For this study's purposes, the H_2 supply is assumed to come from an external source via a pipeline. Ravenna is also known for its chemical manufacturing district, which ensures the availability of essential utilities and waste treatment facilities. Besides operating the CCS hub, Eni also operates a petrochemical plant and a power plant in Ravenna. This creates the potential for industrial symbiosis, enabling on-site decarbonization.

A 50 kta of 85% purity FA plant would require approximately 60 kta of CO_2 and 3 kta of H_2. The anticipated CO_2 supply in Europe will reach 80 Mta by 2030, while the Ravenna CCS Hub will provide 4 Mta by 2027. Regarding H_2, the SouthH_2 project is expected to deliver 4 Mta, and the availability of Hydrogen in Europe is predicted to be 20 Mta by 2030. These projections indicate that the quantities of CO_2 and H_2 are more than adequate.

Process Simulation

Thermodynamic Property Model

The entire process was rigorously simulated using Aspen Plus V12. The properties of the compounds involved in this design were sourced from its database and supplementary literature, which includes thermodynamic binary parameters necessary for characterizing the mixtures within the design (more details can be found in the *Annex* file). For CO synthesis, the Peng-Robinson model was chosen due to the low polarity of the involved compounds. Additionally, the NRTL model was employed for an ethylene glycol/water mixture, serving as a thermal fluid with a low freezing point.

For the MF and FA synthesis system, the UNIQUAC model, coupled with the Hayden O'Connell equation of state (UNIQUAC-HOC) was chosen due to its ability to handle vapor-liquid and liquid-liquid interactions in a non-ideal system with polar compounds. The HOC variant manages the vapour phase dimerization of carboxylic acids such as FA. Furthermore, Henry's law was utilized to account for CO dissolved in the liquid phase, making it suitable for temperatures well above the critical temperature.

Process Design

CO_2 is supplied through the Ravena CCUS hub network pipeline at 25 °C and 35 bar with a certain composition (please refer to the *Annex* file for more details). Pure green H_2 is acquired at 70 °C and 30 bar. Achieving mass-based process yields of 95% for CO_2 and 96% for H_2, the production of FA with an annual output of 50 kta is depicted in the simplified process diagram in **Figure 3**.

The endothermic rWGS reaction occurs in a tubular reactor (R-101) which is simulated after a conversion reactor in Aspen Plus. The chosen catalyst has been assumed to have the same yield at 1.2-1.4 bar, temperature range of 573-600 °C, and H_2-to-CO_2 molar ratio of 2.5 as the case study reported by Jingjing Xu et al. [38]. Although, ideally the reactor operates isothermally, a more pragmatic multi-stage adiabatic approach must be followed because the high temperatures required for the process are difficult to control. Five adiabatic stages with intermediate heating and a combustion heater were used to realistically simulate the process. The number of stages has been set to minimize the adiabatic temperature drop, hence, maintaining the average temperature close to 600 °C.

The produced CO is separated from unreacted feedstock and impurities. Especially challenging is the separation of CO from inert N_2 due to their chemical affinity. COPure™, a chemical adsorption technology, is the ideal design choice and includes the selective adsorption of CO with a $CuAlCl_4$ salt dissolved in toluene. The absorption column (C-101) operates at 27 bar to balance out the slightly lower CO concentration in the feed reflecting the pilot plant data [50]. CO is chemically bound to $CuAlCl_4$ at low temperatures, while other gases are dissolved in toluene. At 90 °C and ambient pressure, the enriched toluene is flashed, while the CO-$CuAlCl_4$ complex is dissociated in a stripper (C-102) at 2 bar and 135 °C [51]. This results in high CO recovery of 98% with a minimum CO purity of 99% [52].

While inert dilution doesn't affect rWGS conversion, high inert levels increase equipment size and capital costs. Hence, a purge stream was added to keep a 5% inert level at the reactor inlet. The pressure difference between the pressurized feedstock and the low-pressure rWGS reaction is used for power generation and in a selective polymeric membrane system (MBR-101) for hydrogen recovery.

A CSTR reactor (R-102) is employed for MF production, operating at a Methanol-to-CO ratio of 5, at 40 bar and 80 °C. An affordable immersed coil cooling system is selected due to its compatibility with the low viscosity process fluid (dynamic viscosity of 0.3 mPa·s). Methanol and CO have single-pass conversions of 14.8% and 74%, respectively, with 100% selectivity towards MF synthesis. Throughout the reaction, the catalyst slowly degrades because of CO_2 poisoning. To maintain the reaction performance, a continuous supply of fresh catalyst, standing at 3% of the total catalyst weight, is introduced into the reactor and a purge stream is included to avoid CO_2 accumulation and catalyst degradation. By upholding a 10% purge ratio, the circulating CO_2 levels are kept at 1.3% mol. Excess of Methanol is retrieved through distillation (C-201) and recycled back into the reactor. The MF stream is further hydrolysed towards FA.

The hydrolysis reaction has the optimum performance in liquid state; thus, the pressure and temperature have been set at 18 bar and 120 °C, respectively [14, 53]. The L/D ratio has been set at 30 to ensure turbulence and, hence, homogeneity in the PFR [54]. The ratio of MF-to-water at the reactor is sustained around 1.8, as dictated by the kinetic model for these operating conditions.

In the first reactor (R-202), 10% of MF reacts with water to produce FA, acting as a catalyst for the next reactor. In the second reactor (R203) -in a single pass- 30.5% of MF is converted to FA with 100% selectivity. The outlet is decompressed, causing partial vaporization of MF and Methanol and cooling of the mixture to prevent re-esterification. Then, MF and Methanol are separated from FA and water, minimizing contact time to avoid FA decomposition [4]. The distillate stream is separated into MF and Methanol, which are recycled to the hydrolysis and carbonylation reactors, respectively. Heavy components are distilled at 3 bar to address the azeotrope between water and FA. An additional Methanol stream of 0.25 kta (1 kmol/h) accounts for losses in the product and purge streams. Further details can be found in the *Annex* file.

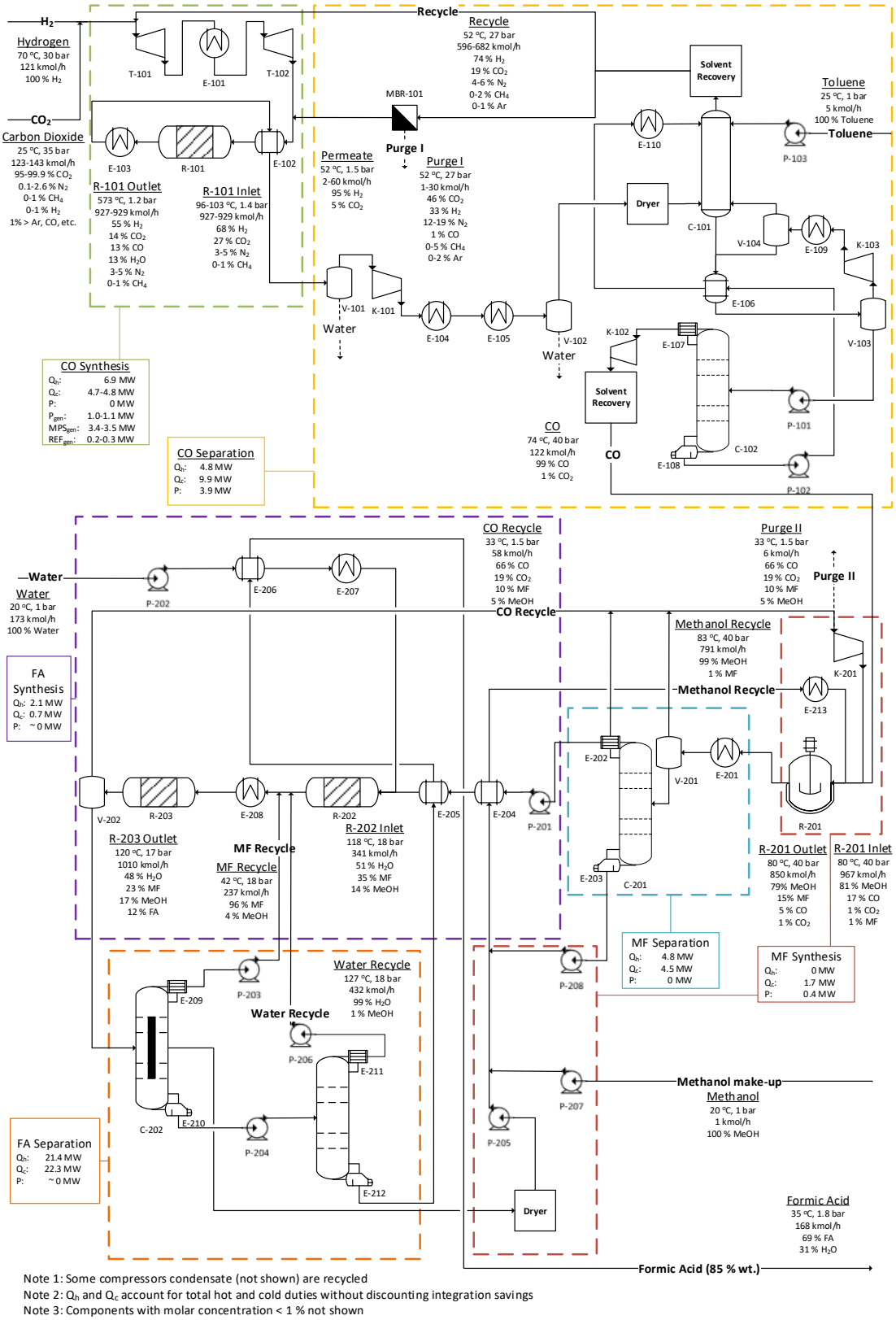

Note 1: Some compressors condensate (not shown) are recycled
Note 2: Q_h and Q_c account for total hot and cold duties without discounting integration savings
Note 3: Components with molar concentration < 1 % not shown

Figure 3: Process flowsheet of the proposed FA synthesis approach from CO_2 and green H_2

Process Intensification

Our work employs the DWC, an intensified distillation technology for simultaneous multi-component separation. While previously assessed as a retrofit for existing FA plants [55], here it is incorporated in a new plant due to its economic viability and impact on capital and operational costs. The separation of MF, Methanol and Water-FA streams requires ambient pressure, and their boiling points differ enough to apply a DWC configuration.

The DWC configuration, simulated in Aspen Plus via a Petlyuk column setup, focuses on separating Methanol, MF, and the FA-H_2O mixture (seen in **Figure 4)**. The energy requirements for the separation a multi-component mixture using a three-product Petlyuk arrangement are on par with those required to separate top/middle or middle/bottom products in a conventional column [56]. The first step in DWC design encompasses the plot of the V_{min} diagram. This graph dictates the minimum vapor flow rates required for effective separation within the column. Despite the feed containing four components, FA and water are grouped together as one component and the DWC design has focused on the separation of Methanol, MF, and the FA-H_2O mixture. In this context, three key separation points have been determined: P_{AB} (separating components A and B), P_{AC} (separating components A and C), and P_{BC} (separating components B and C) where A is MF, B is Methanol, and C the water-FA mixture (illustrated in **Figure 4**). Notably, P_{AC} and P_{BC} are closely located in terms of V_T/T and D/F compared to P_{AB}, implying an easier separation between MF-methanol or water and FA compared to that between MF and methanol. P_{AB} represents the minimum energy requirement, as evidenced by its highest peak in the diagram.

The DWC composition profile, which is displayed in **Figure 5**, thoroughly illustrates how the separation objectives were met. The components of FA and water are mostly found in the lower stages of the pre-fractionator, yet there is a significant concentration of MF and Methanol in the higher stages. A more sophisticated separation procedure takes place towards the main column: MF is successfully pulled off the top, and then Methanol and the FA-water solution are separated further in the middle part. The leftover FA-water mixture simultaneously sinks to the bottom of the column. These profiles highlight how accurately the Petlyuk model simulates DWC.

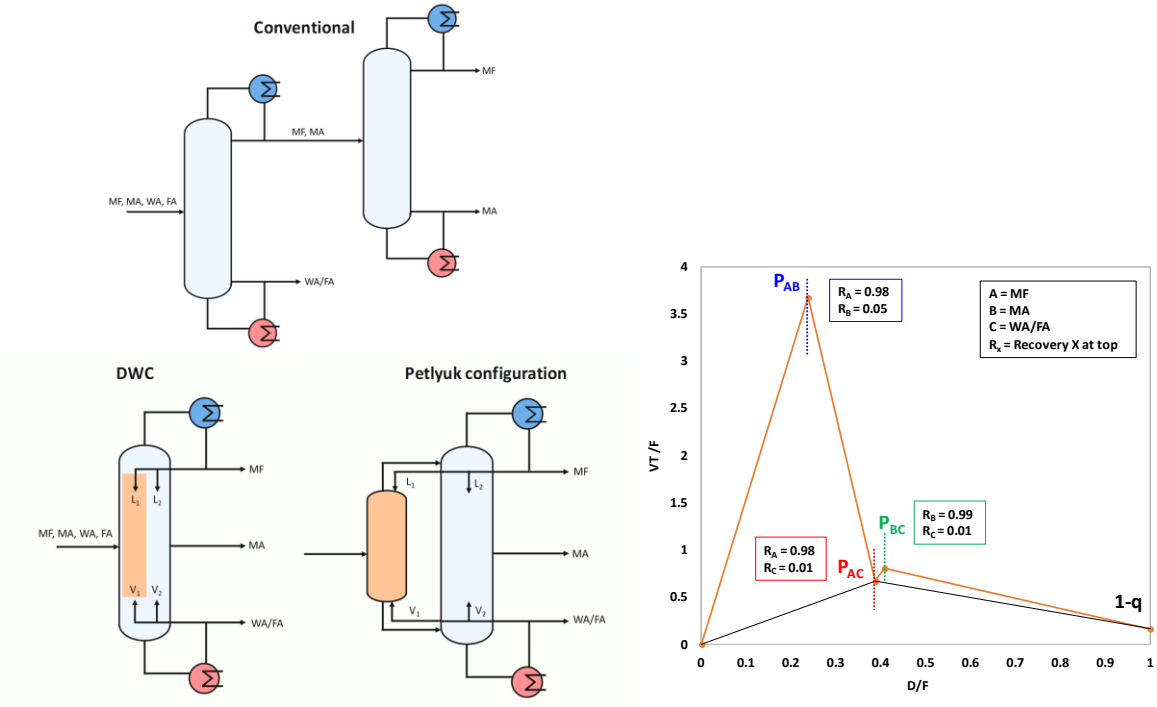

Figure 4: proposed DWC concept in FA separation (left) and V_{min} diagram of DWC feed (right)

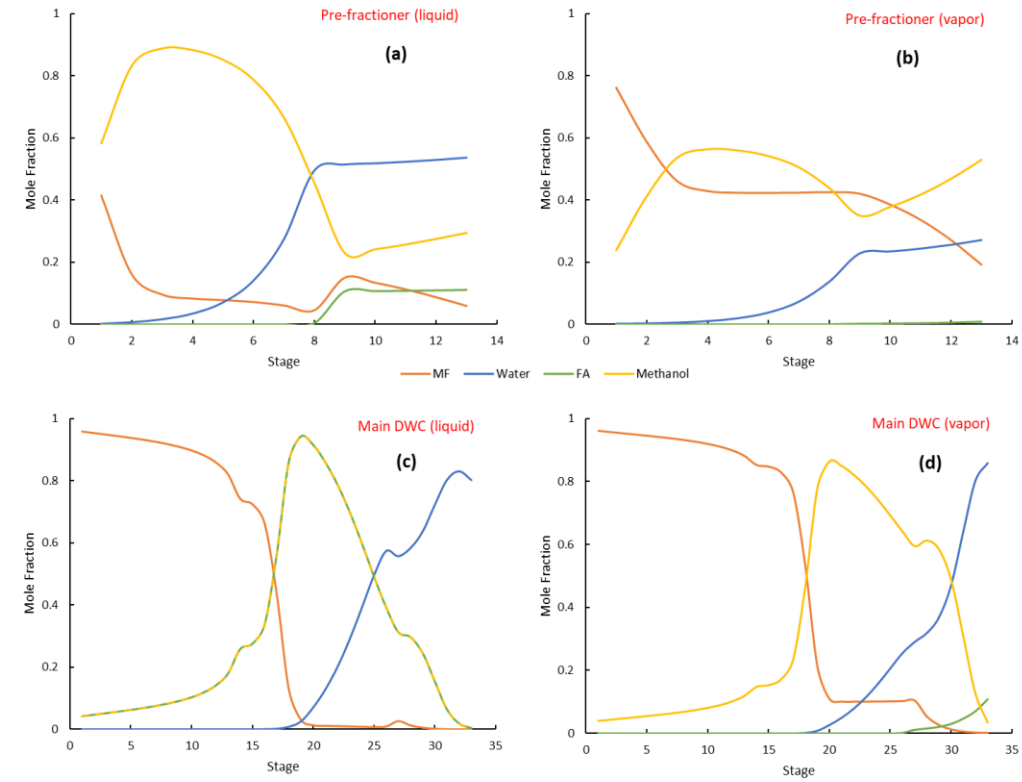

Figure 5: DWC molar composition profiles

Heat Integration

In addition to incorporating PI technology, heat integration was implemented to minimize energy consumption. The high temperature of the CO synthesis reactor outlet stream was valorized by generating medium pressure steam which covers all the duty of the CO separation stripper, and part of the heat required in further sections. Furthermore, the inter-heater between the two turbines used for feedstock depressurization (and power generation) is used to generate a refrigerant which eliminates the requirement for chilled water in the process. Finally, several heat exchangers are implemented throughout the process to economize heat.

Economic Assessment

Capital Investment

An economic forecast for 2030 was conducted, in anticipation of SouthH_2 being operational by that time. The capital expenditure (CAPEX) was initially calculated, comprising fixed capital investment (FCI) and the working capital. These costs, both direct and indirect, are typically a fraction of the bare equipment cost (BEC), which excludes installation, operation, or maintenance costs. BEC is derived from vendor quotes or cost-estimating charts and databases that provide average costs for various types of equipment and is influenced by several factors, including the type, size and capacity of the equipment, construction materials, as well as market conditions. The BEC for 2030 was 18.5 M€, with compressors and columns accounting for about 60% of the total (see **Figure 6**). The CAPEX was computed using the factorial method, resulting in a total capital investment (TCI) of 73.8 M€ in 2030. More details can be found in the *Annex*.

Cost of production

The operational expenditure (OPEX) consists of various components, some derived from the mass and energy balance like raw material and utility costs, and others from the fixed capital investment (FCI) or

plant configuration. The cost of raw materials, especially Hydrogen, significantly impacts the process's sustainability. The cost of raw materials, particularly Hydrogen, is a significant factor in the feasibility of this sustainable process. By 2030, the price of green H_2 is expected to drop to 2500 €/ton [57], subject to regional policies and commitment to the Paris Agreement [58]. The CO_2 price is likely to remain stable. The OPEX for 2030 is projected at 41.8 M€/yr, with raw materials, utilities, and waste treatment as major contributors (see **Figure 6**). More details can be found in the *Annex*.

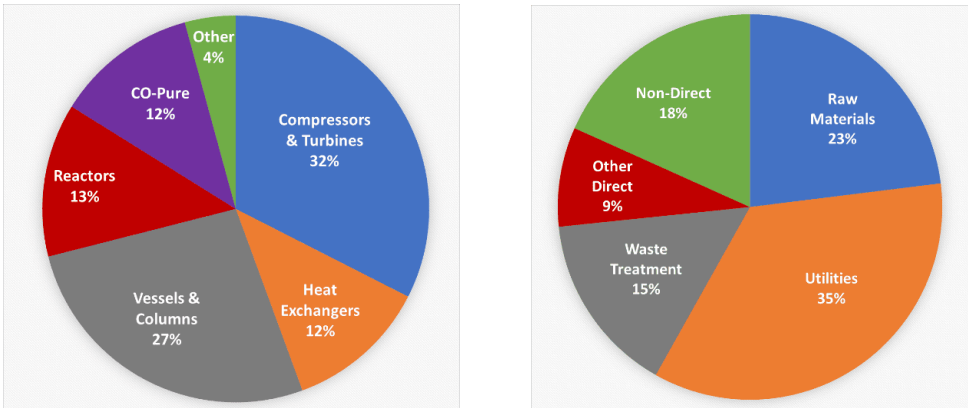

Figure 6: Cost contribution of total BEC (left) and OPEX (right)

Costs Summary

Table 3: Summary of CAPEX and OPEX

CAPEX	**[M€]**	**OPEX**	**[M€/yr]**
Total Direct Plant Cost	50.2	Direct Production Costs	33.8
Total Indirect Plant Cost	14.0	Fixed Charges	4.5
Fixed Capital Investment	64.2	Plant Overhead	1.6
Working Capital	9.6	General Expenses	1.9
Total	**73.8**	**Total**	**41.8**

Revenue and Profit

As for revenues, the price of FA is projected to be around 1200 €/ton in 2030, based on recent prices in Europe of around 1000 €/ton [59], and including an expected rise accounting for inflation and the fact that the conventional process will suffer from increasing costs related to carbon taxes. This study conducted a basic profit and loss analysis using a 10% interest rate and a 20-year plant lifespan. Profit was calculated with the formula below:

$$\text{Profit}\ [€] = \text{Revenues} - \text{Manufacturing cost}, \qquad [8]$$

where manufacturing cost equals the sum of OPEX and annualized capital cost (ACC), calculated as follows:

$$\text{ACC}\left[\frac{€}{\text{yr}}\right] = \text{CAPEX} \times \frac{i(1+i)^n}{(1+i)^{n-1}}, \qquad [9]$$

The estimated profit results in 9.5 M€/yr.

Sensitivity Analysis

Factors like raw materials, utilities, product prices, and plant size were adjusted by ±30% to test profit robustness. Only product price could lead to losses, but current trends don't predict such a low price. Plant size and NG price had moderate influence. Larger plant sizes, up to 100 kta, could enhance economic performance with market assurance. If cheap renewable electricity is available, it could replace natural gas duty by means of electrification of the CO Synthesis reactor heater and column reboilers, reducing energy costs and emissions. See the *Annex* for sensitivity analysis results.

Process Benchmarking Comparison

With fossil fuel-based synthesis

The proposed design has been also compared with the conventional FA production from natural gas, used as our reference case. The KPIs used to evaluate the two cases were obtained from the European Commission's JRC Science for Policy Report [8]. The comparison results are shown in **Table 4**.

The proposed design outperforms the reference case in all KPIs except for cooling water consumption, underlining its future potential towards an eco-friendlier FA production. Specifically, the CO_2 emissions are reduced by half compared to the conventional pathway, mainly due to low direct CO_2 emissions from purge streams whose mass flow rates are relatively low. To assess the total OPEX savings, the cost of each KPI has been quantified according to the utility prices applied in the economic evaluation of this case study, resulting in savings of 13 M€ in OPEX per year.

Table 4: Process performance comparison

KPI	Unit	Reference Case [8]	This Work	Performance (%)
Electrical energy	MWh/t FA	1.55	0.56	-64
Thermal energy (steam)	MJ/kg FA	19.25	15.34	-20
Cooling water usage	tH_2O/t FA	375.50	501.59	34
Process water usage	tH_2O/t FA	0.60	0.50	-17
Total CO_2 emission	tCO_{2eq}/t FA	2.18	1.07	-51

With conventional distillation configuration

The main novelty in this design lies on the environmentally friendlier FA production and the implementation of PI, which aims to reduce capital and energy costs. This is achieved by merging the conventional distillation columns into a single DWC, which is expected to lower equipment cost by decreasing the number of columns and heat exchangers required. An overall CAPEX and OPEX savings summary are presented in **Table 5**. From the utilities point of perspective, the DWC configuration yields significant savings of 8.4 and 7.2 MW regarding the LP steam usage and cooling water duty, respectively. Thus, process intensification results in 12.5% savings in utilities cost. More details can be found in the *Annex*.

Table 5: CAPEX and OPEX savings as well as profitability from DWC implementation

	without DWC	with DWC	Difference
	[M€]		(%)
CAPEX	78.1	73.8	-5.5
OPEX	45.1	41.8	-7.3
Profitability	5.7	9.5	66.7
Type	**[M€]**		**(%)**
Heat exchangers	1.52	0.95	-38
Distillation columns	3.86	3.37	-13
Utilities	15.02	13.18	-12
Maintenance	2.04	1.93	-5
Utilities	**Energy Consumption [MW]**		**(%)**
CW	35.6	28.4	-20
LP Steam	19.8	11.4	-42
MP Steam	13.9	15.3	10

Conclusions

This work presents an innovative design for producing 50 kta of FA using captured CO_2. The DWC configuration and heat integration result in an overall 19% energy reduction compared to traditional methods, leading to an energy intensity of 21.8 MJ/kg of FA. Moreover, the process halves $CO_{2(eq)}$ emissions to 1.07 kg CO_{2eq}/kg_{FA} and aligns with future environmental standards. The economic evaluation indicates positive returns by 2030, although the estimated profit of 9.5 M€/yr is sensitive to factors like product and natural gas prices. Integration into larger chemical plant complex could leverage process synergies and reduce utility costs, whereas incorporating a membrane reactor could further improve cost, energy, and material efficiency by facilitating continuous product removal and shifting the equilibrium towards a higher CO yield. Nevertheless, our design supplemented by DWC technology, offers a sustainable and energy-efficient FA production method ready for industrial incorporation.

Acknowledgements

Our team extends its deepest gratitude to Professor Tony Kiss for his instrumental support and guidance through the project. His expertise and dedication have truly enriched our learning experience. Moreover, we would like to express our sincere appreciation to Dr.ir. Farzad Mousazadeh. His meticulous attention to detail and invaluable suggestions have significantly enhanced the quality of our report.

References

1. *Renewable Energy Directive*. 2023 20 Feb 2024]; Available from: https://energy.ec.europa.eu/topics/renewable-energy/renewable-energy-directive-targets-and-rules/renewable-energy-directive_en.
2. Olah, G.A., G.K.S. Prakash, and A. Goeppert, *Anthropogenic Chemical Carbon Cycle for a Sustainable Future.* Journal of the American Chemical Society, 2011. **133**(33): p. 12881-12898.
3. ChemAnalyst. *Formic Acid Price Trend and Forecast*. 2023 [cited 2023 1 March]; Available from: https://www.chemanalyst.com/Pricing-data/formic-acid-1242.
4. Hietala, J., et al., *Formic Acid*, in *Ullmann's Encyclopedia of Industrial Chemistry*. 2016, Wiley. p. 1-22.
5. Chen, X., Y. Liu, and J. Wu, *Sustainable production of formic acid from biomass and carbon dioxide.* Molecular Catalysis, 2020. **483**: p. 110716.
6. Bankar, B.D., et al., *Direct hydrogenation of CO2 to formic acid using Ru supported Co3O4 oxide as an efficient heterogeneous catalyst.* Molecular Catalysis, 2023. **535**: p. 112875.
7. Álvarez, A., et al., *Challenges in the Greener Production of Formates/Formic Acid, Methanol, and DME by Heterogeneously Catalyzed CO2 Hydrogenation Processes.* Chemical Reviews, 2017. **117**(14): p. 9804-9838.
8. Pérez-Fortes, M., et al., *Formic acid synthesis using CO2 as raw material: Techno-economic and environmental evaluation and market potential.* International Journal of Hydrogen Energy, 2016. **41**(37): p. 16444-16462.
9. Nishikawa, E. *CO2 conversion & utilization pathways: Techno-economic insights*. 2022 [cited 2023 15 March]; Available from: https://www.prescouter.com/2022/04/co2-conversion-utilization-pathways/.
10. Barbera, E., et al., *Hydrogenation to convert CO2 to C1 chemicals: Technical comparison of different alternatives by process simulation.* The Canadian Journal of Chemical Engineering, 2020. **98**(9): p. 1893-1906.
11. Yang, L., *CO2 conversion via reverse water-gas shift using multicomponent catalysts*, L. Pastor Perez and T. Ramirez Reina, Editors. 2021, University of Surrey.
12. ChemAnalyst. 2023 [cited 2023 1 March]; Available from: https://www.chemanalyst.com/.
13. Zhong, Z., U. Etim, and Y. Song, *Improving the Cu/ZnO-Based Catalysts for Carbon Dioxide Hydrogenation to Methanol, and the Use of Methanol As a Renewable Energy Storage Media.* Frontiers in Energy Research, 2020. **8**.
14. Chua, W.X., et al., *Design and optimization of Kemira-Leonard process for formic acid production.* Chemical Engineering Science: X, 2019. **2**: p. 100021.
15. Reutemann, W. and H. Kieczka, *Formic acid.* Ullmann's encyclopedia of industrial chemistry, 2011. **16**: p. 67-82.

16. Miranda, J.C.d.C., et al., *Process design and evaluation of syngas-to-ethanol conversion plants.* Journal of Cleaner Production, 2020. **269**: p. 122078.
17. ICIS, *Chemical Prices*. 2006.
18. Nicholson, S.R., et al., *Manufacturing Energy and Greenhouse Gas Emissions Associated with United States Consumption of Organic Petrochemicals.* ACS Sustainable Chemistry & Engineering, 2023. **11**(6): p. 2198-2208.
19. Rossi, G.E., et al., *Phosgene formation via carbon monoxide and dichlorine reaction over an activated carbon catalyst: Reaction kinetics and mass balance relationships.* Applied Catalysis A: General, 2020. **602**: p. 117688.
20. Dimian, A.C. and A.A. Kiss, *Novel energy efficient process for acetic acid production by methanol carbonylation.* Chemical Engineering Research and Design, 2020. **159**: p. 1-12.
21. Kalck, P., C. Le Berre, and P. Serp, *Recent advances in the methanol carbonylation reaction into acetic acid.* Coordination Chemistry Reviews, 2020. **402**: p. 213078.
22. Isla, M.A., H.A. Irazoqui, and C.M. Genoud, *Simulation of a urea synthesis reactor. 1. Thermodynamic framework.* Industrial & Engineering Chemistry Research, 1993. **32**(11): p. 2662-2670.
23. Analytic, B. 2023 [cited 2023 1 March]; Available from: https://businessanalytiq.com/.
24. Michailos, S., et al., *Dimethyl ether synthesis via captured CO2 hydrogenation within the power to liquids concept: A techno-economic assessment.* Energy Conversion and Management, 2019. **184**: p. 262-276.
25. Brunetti, A., et al., *Methanol Conversion to Dimethyl Ether in Catalytic Zeolite Membrane Reactors.* ACS Sustainable Chemistry & Engineering, 2020. **8**(28): p. 10471-10479.
26. Kongpanna, P., et al., *Techno-economic evaluation of different CO2-based processes for dimethyl carbonate production.* Chemical Engineering Research and Design, 2015. **93**: p. 496-510.
27. Kuenen, H.J., et al., *Techno-economic evaluation of the direct conversion of CO2 to dimethyl carbonate using catalytic membrane reactors.* Computers & Chemical Engineering, 2016. **86**: p. 136-147.
28. Rossberg, M., et al., *Chlorinated Hydrocarbons*, in *Ullmann's Encyclopedia of Industrial Chemistry*.
29. Kiss, A., et al., *Novel efficient process for methanol synthesis by CO2 hydrogenation.* Chemical Engineering Journal, 2016. **284**: p. 260-269.
30. Bown, R., et al., *Identifying Commercial Opportunities for the Reverse Water Gas Shift Reaction.* Energy Technology, 2021. **9**.
31. Reutemann, W. and H. Kieczka, *Formic Acid*, in *Ullmann's Encyclopedia of Industrial Chemistry*.
32. Kaiser, D., et al., *Conversion of Green Methanol to Methyl Formate.* Catalysts, 2021. **11**(7): p. 869.
33. Reutemann, W. and H. Kieczka, *Formic Acid*, in *Ullmann's Encyclopedia of Industrial Chemistry*, V.C.H.V.G. Wiley and K. Co, Editors. 2000, Wiley-VCH Verlag GmbH & Co. KGaA: Weinheim, Germany. p. a12_013.
34. Nelson, W.L. and C.J. Engelder, *The Thermal Decomposition of Formic Acid.* The Journal of Physical Chemistry, 1926. **30**(4): p. 470-475.
35. Pasek, J., J. Trejbal, and P. Roose, *Process of formic acid production by hydrolysis of methyl formate*, U. European, Editor. 2014, Taminco BV.
36. Roy, S., A. Cherevotan, and S.C. Peter, *Thermochemical CO2 Hydrogenation to Single Carbon Products: Scientific and Technological Challenges.* ACS Energy Letters, 2018. **3**(8): p. 1938-1966.
37. Porosoff, M.D., et al., *Molybdenum Carbide as Alternative Catalysts to Precious Metals for Highly Selective Reduction of CO2 to CO.* Angewandte Chemie International Edition, 2014. **53**(26): p. 6705-6709.
38. Xu, J., et al., *Highly active K-promoted Cu/β-Mo2C catalysts for reverse water gas shift reaction: Effect of potassium.* Molecular Catalysis, 2021. **516**: p. 111954.
39. Leonard, J.D., *Preparation of formic acid by hydrolysis of methyl formate*, S. United, Editor. 1981, Leonard Jackson D.
40. Jogunola, O., et al., *Reversible Autocatalytic Hydrolysis of Alkyl Formate: Kinetic and Reactor Modeling.* Industrial & Engineering Chemistry Research, 2010. **49**(9): p. 4099-4106.
41. Jogunola, O., et al., *Kinetic studies of alkyl formate hydrolysis using formic acid as a catalyst.* Journal of Chemical Technology & Biotechnology, 2012. **87**(2): p. 286-293.
42. Skoog, D., *Analytical chemistry'all introduction.* US: Saunders College Publishing, 2000.
43. Burghaus, U., *Surface chemistry of CO2 – Adsorption of carbon dioxide on clean surfaces at ultrahigh vacuum.* Progress in Surface Science, 2014. **89**(2): p. 161-217.

44. Zhang, X., et al., *Highly Dispersed Copper over β-Mo2C as an Efficient and Stable Catalyst for the Reverse Water Gas Shift (RWGS) Reaction.* ACS Catalysis, 2017. **7**(1): p. 912-918.
45. *Sharing insights elevates their impact.* S&P Global.
46. *Our activities in Ravenna.* 2024.
47. *Plenitude completes construction of Ravenna Ponticelle photovoltaic plant.*
48. *Saipem, protagonist in offshore wind, will develop a wind farm in Italy | Saipem.* 2024.
49. *SoutH2 - The initiative.* 2024.
50. Sato, T., et al., *CHEMICAL REACTION OF CARBON MONOXIDE WITH COPPER(I)-TETRACHLOROALUMINATE(III)-AROMATIC HYDROCARBON SOLUTIONS-EQUILIBRIUM AND KINETICS.* Journal of Chemical Engineering of Japan, 1988. **21**(2): p. 192-198.
51. Go, Y.-T., et al., *Mathematical Modeling and Simulation of Carbon Monoxide Absorption Column for Blast Furnace Gas and Linz–Donawitz Gas Separation by COSORB Process.* JOURNAL OF CHEMICAL ENGINEERING OF JAPAN, 2019. **52**: p. 439-446.
52. Bierhals, J., *Carbon Monoxide*, in *Ullmann's Encyclopedia of Industrial Chemistry*.
53. Jogunola, O., et al., *Kinetics of Methyl Formate Hydrolysis in the Absence and Presence of a Complexing Agent.* Industrial & Engineering Chemistry Research, 2011. **50**(1): p. 267-276.
54. Sauer, J., N. Dahmen, and E. Henrich, *Tubular Plug Flow Reactors*. 2013. p. 1-23.
55. da Cunha, S., G.P. Rangaiah, and K. Hidajat, *Design, Optimization, and Retrofit of the Formic Acid Process I: Base Case Design and Dividing-Wall Column Retrofit.* Industrial & Engineering Chemistry Research, 2018. **57**(29): p. 9554-9570.
56. Halvorsen, I.J. and S. Skogestad, *Minimum Energy Consumption in Multicomponent Distillation. 2. Three-Product Petlyuk Arrangements.* Industrial & Engineering Chemistry Research, 2003. **42**(3): p. 605-615.
57. Statista. *Green hydrogen cost breakdown scenario 2030*. 2023; Available from: https://www.statista.com/statistics/1220812/global-hydrogen-production-cost-forecast-by-scenario/#:~:text=In%202020%2C%20renewable%20hydrogen%20costs%20amounted%20to%20six,dollars%20per%20kilogram%20of%20hydrogen%20by%202030%2C%20respectively.
58. UNFCCC. *The Paris Agreement*. Available from: https://unfccc.int/process-and-meetings/the-paris-agreement#:~:text=The%20Paris%20Agreement%20is%20a%20legally%20binding%20international,It%20entered%20into%20force%20on%204%20November%202016.
59. Chemanalyst. *Formic Acid Price, Trend and Forecast*. 2023; Available from: https://www.chemanalyst.com/Pricing-data/formic-acid-1242.

Transforming CO_2 into Formic Acid: An Eco-Efficient Design in Italy

Annexes

A. Thermodynamic Parameters

CO Synthesis and Separation

The binary parameters used in Peng Robinson equation are the following:

Table A.1: Peng Robinson binary parameters (PRKBV)

Component *i*	CO	CO	CO_2	CO_2	CO_2	CO_2	H_2	H_2	N_2
Component *j*	H_2	N_2	H_2	H_2O	N_2	TOL	N_2	TOL	TOL
a_{ij}	0.0919	0.0307	-0.1622	0.12	-0.017	0.1056	0.103	-0.1114	0.19701
b_{ij}	0	0	0	0	0	0	0	0	0
c_{ij}	0	0	0	0	0	0	0	0	0

All data were retrieved from Aspen Plus V12 EOS-LIT database, except H_2/TOL and N_2/TOL which were regressed from NIST datasets ([1, 2]). CO/TOL parameters were not available, but this is not critical since COPure™ technology's known performance suggests minimal impact from toluene absorption compared to CO chemisorption by the salt. The binary parameters used in the NRTL equation for the Ethylene Glycol/Water solution are:

Table A.2: NRTL binary parameters (NRTL-1)

Component *i*	Water
Component *j*	Ethylene Glycol
a_{ij}	0.3479
a_{ji}	-0.0567
b_{ij}	34.8234
b_{ji}	-147.1373
c_{ij}	0.3

MF and FA Synthesis and Separation

The binary parameters used in UNIQUAC equation are the following:

Table A.3: UNIQUAC binary parameters

Component *i*	MF	MF	MF	Water	Methanol	Water
Component *j*	Water	Methanol	FA	Methanol	FA	FA
a_{ij}	0	0	1.46	2.06	0	1.9779
a_{ji}	0	0	1.86	-3.15	0	-2.5846
b_{ij}	-434.24	-15.2	-471.54	-219.04	366.61	920.795
b_{ji}	-99.35	-301.76	132.65	575.68	-615.9	-539.679
d_{ij}	0	0	0	-0.007	0	0
d_{ij}	0	0	0	0.006	0	0

All data were retrieved from literature [3], except FA-Water parameters which have been retrieved from Aspen Plus V12 VLE-HOC database, as they better describe the expected azeotropic composition. The binary parameters for Henry's Law are the following:

Table A.4: Henry's Law binary parameters

Mixture	A^H_{ij}	B^H_{ij}	C^H_{ij}	Reference
CO + Methanol	4.21187	1144.4	0	APV120 HENRY-AP databank
CO + MF	2.92	1721.0	0	Liu 1988 [4]
CO + Water	171.775	-8296.75	-23.3372	APV120 BINARY databank

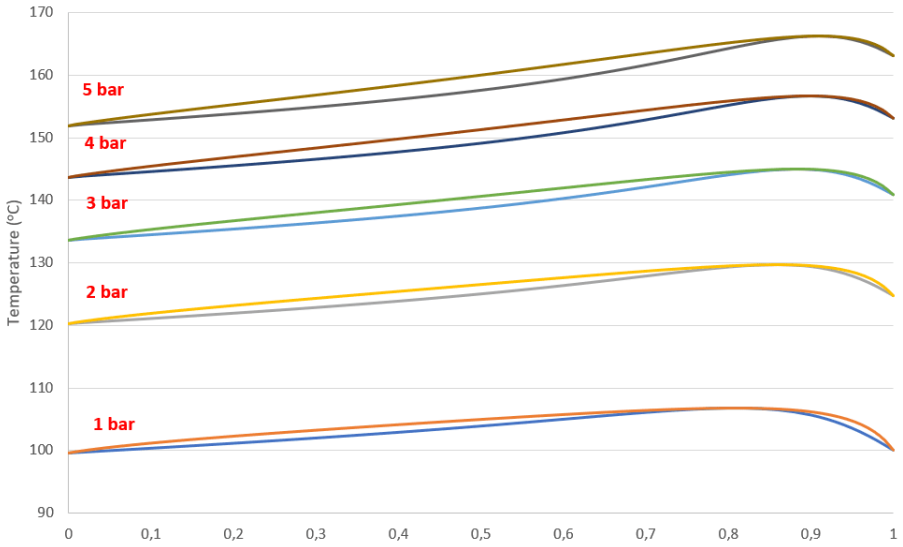

Figure A-1: T-xy graphs for FA-water mixture in different pressures (obtained from Aspen Plus)

B. Raw Material Specification

Two fresh CO_2 feedstock compositions were considered: a limit case and a typical case.

- Limit case: This represents the minimum required specifications for pipeline transport of CO_2. These specifications are indicated in this work and act as a quality threshold.
- Base case: This reflects the typical composition of CO_2 obtained from post-combustion capture. As noted by Abbas et al. [5], typical post-combustion CO_2 MEA systems (which can be assumed to be Ravenna hub suppliers) outperform in many of these specifications with the exception of water and oxygen content. These impurities are typically removed to meet the limit case requirements.

Table B.1: Limit and typical composition of CO_2 feedstock [5]

Component (mol base)	Limit	Typical
CO_2	≥ 95%	≥ 99%
H_2	≤ 0.75%	≤ 0.75%
N_2	≤ 2.4%	≤ 0.13%
Ar	≤ 0.4%	≤ 25 ppm
CH_4	≤ 1%	-
CO	≤ 750 ppm	-
O_2	≤ 40 ppm	-
Other	≤ 0.2%	-
SUM of impurities	≤ 4%	≤ 1%

For this reason, a CO_2 feed with 99.87% CO_2 and 0.13% of N_2 as the only impurity will be considered for

the base case, while the limit values will be only considered to size the necessary purge in this extreme event.

The hydrogen input specification is derived from the $SoutH_2$ pipeline as dry Hydrogen (water not present) and is assumed to be 99.99% pure (0.01% is Oxygen).

C. Equipment Sizing

The results of the sizing of each equipment are presented in the following tables:

Table C.1: Sizing overview of reactors [6]

EQUIPMENT	R-101	R-201	R-202	R-203
Pressure [bar]	1.4/1.2	40/40	17.5/16.5	17.5/16.6
Temperature [°C]	600/600	80/80	120/120	120/120
Diameter [m]	0.03	3.63	0.5	0.67
L or H [m]	9	5.45	15	20
Material	SS316	SS304	Alloy 904L	Alloy 904L

Table C.2: Sizing overview of columns [6]

EQUIPMENT	C-101	C-102	C-201	C-202	C-203
Pressure [bar]	25.5/27	1.8/1.9	4.8/5	1.4/1.5	2.5/3
Temperature [°C]	51.9/38.5	80/80	35.6/111.7	40.8/111.6	111.7/141.5
Diameter [m]	0.96	1.80	1.3	2.4	2.3
L or H [m]	23.5	4.3	8.5	20.2	15.2
Packing/Tray type	Pall	Sieve	Sieve	Sieve	Sieve
Number of trays	40	7	16	31	25
Feed stage	1/40	5	10	14	14
Reflux ratio	-	1.00	1.26	3.30	2.06
Reboiler type	-	Kettle	Kettle	Kettle	Kettle
Condenser type	-	Shell & tube	Shell & tube	Shell & tube	Shell & tube
Materials	SS304	CS	SS304	Alloy 904L	Alloy 904L

Table C.3: Sizing overview of vessels [6]

EQUIPMENT	V-101	V-102	V-103	V-104	V-105	V-201	V-202	V-204	V-205
Pressure [bar]	1	27	2.9	1.8	27	40	4.8	1.4	2.5
Temperature [°C]	41.2	12	100	39.8	12	35	35.6	40.8	125.9
Diameter [m]	1.65	0.68	0.52	0.52	0.17	1.35	1.15	1.00	0.84
L or H [m]	2.51	1.02	2.07	1.55	0.36	4.06	3.44	2.98	2.51
Materials	CS	CS	CS	CS	CS	SS304	CS	Alloy 904L	Alloy 904L

Table C.4: Sizing overview of heat exchangers [6]

EQUIPMENT	**E-101**	**E-102**	**E-103**	**E-104**	**E-105**
Type	Shell & Tube	Shell & Tube	Kettle Reboiler	Shell & Tube	Shell & Tube
Number (Series/parallel)	1/1	1/1	1/1	1/1	1/1
Substance					
Shell	Process F.	Process F.	MP Steam (generation)	CW	EG/WTR 60 wt%
Tube	EG/WTR 60 wt%	Process F.	Process F.	Process F.	Process F.
Duty [kW]	250	1275	-3489	-642	-178
Heat exchange area [m^2]	35.7	127.5	167.0	28.8	26.3
			Temp. IN/OUT [°C]		
Shell:	10/0	-56/102.6	159/160	20/30	0/10
Tube:	-33.5/-1	170/50	573/170	122.8/35	35/12
			Pressure IN/OUT [bar]		
Shell:	1.5/1.0	1.5/1.4	6.0/5.5	3/2.5	1.5/1.0
Tube:	6/5.9	1.1/1.0	1.2/1.1	27.2/27.1	27.1/27
			Materials		
Shell:	SS316	SS316	CS	CS	SS316
Tube:	SS316	SS316	SS316	SS316	SS316
EQUIPMENT	**E-106**	**E-107**	**E-108**	**E-109**	**E-110**
Type	Shell & Tube	Shell & Tube	Kettle	Shell & Tube	Shell & Tube
Number (Series/parallel)	1/1	1/1	1/1	1/1	1/1
Substance					
Shell	Process F.	CW	Process F.	EG/WTR 60 wt%	CW
Tube	Process F.	Process F.	MP steam	Process F.	Process F.
Duty [kW]	1823	1653	2987	-39	500
Heat exchange area [m^2]	423.2	140.6	113.3	5.1	15.9
			Temp. IN/OUT [°C]		
Shell:	38.2/100	20/30	134.6/134.7	0/10	20/30
Tube:	135.4/70.2	109.1/48	160/159	110.6/12	70.2/50
			Pressure IN/OUT [bar]		
Shell:	3.4/2.9	3/2.5	1.8/1.8	1.5/1.0	3/2.5
Tube:	28/27.5	1.8/1.8	6.1/6	27.1/27	27.5/27
			Materials		
Shell:	CS	CS	CS	SS316	CS
Tube:	CS	CS	CS	SS316	CS

EQUIPMENT	**E-201**	**E-202**	**E-203**	**E-204**	**E-205**
Type	Shell & Tube	Shell & Tube	Kettle Reboiler	Shell & Tube	Shell & Tube
Number (Series/parallel)	1/1	1/1	1/1	1/1	1/1
Substance					
Shell	CW	Profess F.	Process F.	Process F.	Process F.
Tube	Process F.	CW	LP steam	Process F.	Process F.
Duty [kW]	-998	-3466	4759	253	195
Heat exchange area [m^2]	43.4	133.9	330.3	10.4	44.5
			Temp. IN/OUT [°C]		
Shell:	20.0/30.0	83.2/35.6	111.5/111.7	37.0/84.3	141.5/94.3
Tube:	69.4/35.0	20.0/30.0	125.0/124.0	104.8/94.3	84.3/117.0
			Pressure IN/OUT [bar]		
Shell:	3.0/2.5	4.9/4.9	5.0/5.0	19.0/18.5	2.8/2.3
Tube:	5.5/5.0	3.0/2.5	2.3/2.3	41.0/40.5	18.5/18.0
			Materials		
Shell:	CS	CS	SS304	CS	SS904L
Tube:	SS304	CS	SS304	SS304	SS904L
EQUIPMENT	**E-206**	**E-207**	**E-208**	**E-209**	**E-210**
Type	Shell & Tube	Shell & Tube	Shell & Tube	Shell & Tube	Kettle Reboiler
Number (Series/parallel)	1/1	1/1	1/1	1/1	1/1
Substance					
Shell	Process F.	Process F.	MP Steam	CW	Process F.
Tube	Process F.	MP Steam	Process F.	Process F.	LP steam
Duty [kW]	202	229	738	-7832	6659
Heat exchange area [m^2]	90.1	4.8	13.8	558.7	405.3
			Temp. IN/OUT [°C]		
Shell:	21.1/78.4	78.4/140.0	160.0/159	20.0/30.0	108.4/111.6
Tube:	94.3/35.0	160.0/159	95.4/120.0	40.8/40.8	125.0/124.0
			Pressure IN/OUT [bar]		
Shell:	19.0/18.5	18.5/18.0	6.2/6.0	3.0/2.5	1.4/1.4
Tube:	2.3/1.8	6.2/6.0	18.0/17.5	1.4/1.4	2.3/2.3
			Materials		
Shell:	SS904L	CS	CS	CS	SS904L
Tube:	SS904L	CS	SS904L	SS904L	SS904L

EQUIPMENT	E-211	E-212	E-213
Type	Shell & Tube	Kettle Reboiler	Shell & Tube
Number (Series/parallel)	1/2	1/1	1/1
Substance			
Shell	CW	Process F.	CW
Tube	Process F.	MP steam	Process F.
Duty [kW]	-14436	14747	-261
Heat exchange area [m^2]	108.4	671.6	4.2
	Temp. IN/OUT [°C]		
Shell:	20.0/30.0	141/141	20.0/30.0
Tube:	127.5/125.9	160.0/159	94.3/83.0
	Pressure IN/OUT [bar]		
Shell:	3.0/2.5	2.8/2.8	3.0/2.5
Tube:	2.5/2.5	6.2/6.0	40.5/40.0
	Materials		
Shell:	CS	SS904L	CS
Tube:	SS904L	SS904L	SS304

Table C.5: Sizing overview of pumps, compressors and turbines [6]

EQUIPMENT	P-101	P-102	P-103	P-104	P-201
Type	Centrifugal		Multi-Stage	Centrifugal	
Amount	2	2	2	2	2
Temperature IN/OUT [°C]	90 / 90	135 / 135	134 / 136	25 / 30	36 / 37
Pressure Suct./Disch. [bar]	1.0 / 2.0	1.8 / 3.4	3.4 / 28.0	1.0 / 27.0	4.84 / 19
Power (kW)	2.71	4.40	69.94	1.42	9.04
Materials	CS	CS	CS	CS	SS304
EQUIPMENT	**P-202**	**P-203**	**P-204**	**P-205**	**P-206**
Type			Centrifugal		
Amount	2	2	2	2	2
Temperature IN/OUT [°C]	20 / 21	112 / 112	41 / 42	126 / 127	67 / 71
Pressure Suct./Disch. [bar]	1 / 19	1.4 / 3	1.4 / 18	2.5 / 18	1.4 / 41
Power (kW)	5.3	1.5	6.8	0.071	21.7
Materials	Cast iron	Alloy 904L	SS304	SS316	SS304

EQUIPMENT	P-207	P-208	P-209	P-210	K-101
Type	Centrifugal		Reciprocating		Centrifugal
Amount	2	2	2	2	2
Temperature IN/OUT [°C]	112 / 114	20 / 26	40 / 45	40 / 44	42 / 112
Pressure Suct./Disch. [bar]	5 / 41	1 / 41	7.2 / 41	17.1 / 41	1.0 / 27.2
Power (kW)	51.4	1.15	0.07	0.43	4357.6
Materials	SS304	CS	SS304	SS304	CS
EQUIPMENT	**K-102**	**K-103**	**K-201**	**T-101**	**T-102**
Type		Centrifugal			
Amount	2	2	2	2	2
Temperature IN/OUT [°C]	40 / 74	90 / 111	33 / 138	45 / -34	-1 / -63
Pressure Suct./Disch. [bar]	1.8 / 40.0	1.0 / 27.1	1.5 / 40	26.6 / 6.0	6.0 / 1.3
Power (kW)	610.7	252.2	221.4	-594.2	-474.6
Materials	CS	CS	CS	CS	CS

Sizing and cost calculations of the CO separation (COPure^{TM}) and the membrane were done from [7] and [8].

D. Utility condition and consumption

The utility types and conditions used as design basis are shown in **Table D.1** below. The utilities consumed in each equipment was also documented in **Table D.2**.

Table D.1: Utilities type and condition

Utilities	Inlet Condition	Outlet Condition
Cooling Water	20 °C; 3 bar	30 °C; 2.5 bar
Ethylene Glycol/Water (60/40 %wt)	0 °C/10 °C; 1.5 bar	10 °C/0 °C; 1 bar
Natural Gas	-	-
Low Pressure Steam (LPS)	125 °C; V_f = 1	124 °C; V_f = 0
Medium Pressure Steam (MPS)	160°C; V_f = 1	159 °C; V_f = 0
Electricity	-	-

Table D.2: Utility requirements in each process unit

Equipment	Utilities Type	Heating Duty [kW]	Cooling Duty [kW]	Power [kW]	Energy Generation [kW]
CO Synthesis					
E-101	Refrigerant				250
E-102	Process Stream	1270			
R-101	Natural Gas	5420			
T-101	-				565
T-102	-				452
TOTAL		6690			1267

Equipment	Utilities Type	Heating Duty [kW]	Cooling Duty [kW]	Power [kW]	Energy Generation [kW]
CO Separation					
E-102	Process Stream		1270		
E-103	MPS				3449
E-104	CW		640		
E-105	Refrigerant		177		
E-106	Process Stream	1818	1818		
E-107	CW		1653		
E-108	MPS	2988			
E-109	Refrigerant		38		
E-110	CW		508		
K-101	Power		3882	3353	
K-103	Power		631	195	
P-101	Power			3	
P-102	Power			5	
P-103	Power			75	
P-104	Power			2	
TOTAL		4806	10617	3633	3449
MF Synthesis					
E-204A	Process Stream		253		
E-212	MPS		261		
K-102	Power		514	469	
k-201	Power		207	233	
P-206	Power			10	
P-207	Power			23	
P-208	Power			54	
P-209	Power			1	
P-210	Power			1	
R-201	CW		1025	89	
TOTAL			2260	880	
MF Separation					
E-201	CW		998		
E-202	CW		3467		
E-203	LPS	4759			
TOTAL		4759	4465		

Equipment	Utilities Type	Heating Duty [kW]	Cooling Duty [kW]	Power [kW]	Energy Generation [kW]
FA Synthesis					
E-204A	Process Stream	253			
E-204B	Process Stream	195			
E-205	MPS	229			
E-206	MPS	738			
R-203	CW		193		
P-201	Power			10	
P-202	Power			6	
P-204	Power			15	
P-205	Power			10	
E-211	Process Stream	202			
TOTAL		1617	193	41	
FA Separation					
E-204B	Process Stream		195		
E-207	CW		7832		
E-208	LPS	6659			
E-209	CW		14436		
E-210	MPS	14747			
E-211	Process Stream		202		
P-203	Power			2	
TOTAL		21406	22665	2	

E. DWC Optimization

Optimization was done by performing sensitivity analysis on the effect of the pre-fractionator column's height to the main column's reboiler duty, FA-water distillation column's duty, methanol purity, and MF purity. The total reboiler duty was found to be the main factor that influences the decision making as it has a significant impact on the process's energy needs. To obtain consistent results, the distillate rate was set equal to the MF recycle rate in the non-DWC setup, with r_V and r_L set to 0.2.

Pre-fractionator Heigh optimization

The reference point of this pre-fractionator height optimization was the height of C-201 distillation column in non-DWC case (13 stages). Negative number refers to a smaller number of stages and positive number refers to a greater number of stages. The best result was observed in reference case without significant difference in final FA productivity nor MF-MeOH purity.

Table E.1: Pre-fractionator height optimization parameters

N*	Duty Main Reboiler [MW]	Duty FA Reboiler [MW]	Total Reboiler Duty [MW]	MF Purity	Methanol Purity	FA rate [kmol/h]
-6	17.91	11.91	29.82	0.95	0.97	167.1
-4	16.95	11.53	28.48	0.95	0.97	166.8
-2	16.79	10.93	27.72	0.95	0.97	168.1
-1	16.45	10.63	27.08	0.94	0.97	167.4
0 (*13*)	16.35	10.56	26.91	0.93	0.97	166.9
1	16.48	10.65	27.13	0.94	0.97	167.5
2	16.49	10.66	27.15	0.94	0.97	167.6
4	16.51	10.67	27.19	0.94	0.97	167.7

*Evaluated from initial stage number 13

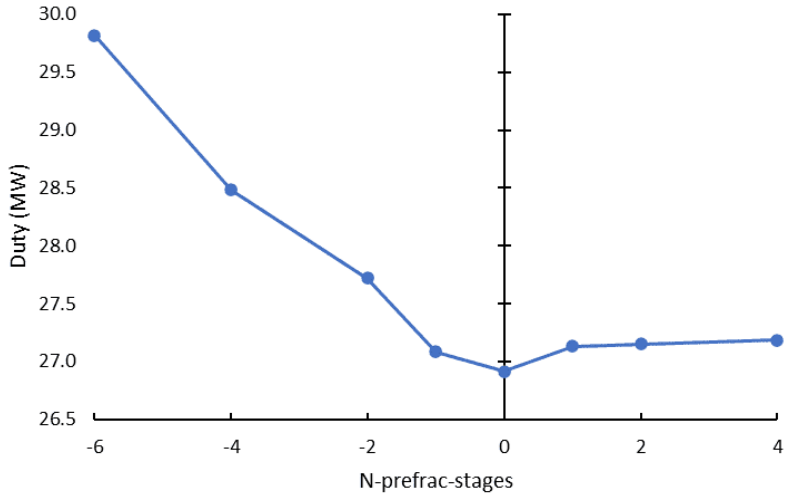

Figure E-1: Pre-fractionator height correlation to total reboiler duty

Pre-fractionator feed stage optimization

This optimization affects the initial feeding position at the pre-fractionator column. The best result was observed when feeding from the 9th stage of pre-fractionator without significant difference in final FA productivity nor MF-MeOH purity.

Table E.2: Feed stage optimization parameters

N_f	Duty Main Reboiler [MW]	Duty FA Reboiler [MW]	Total Reboiler Duty [MW]	MF Purity	Methanol Purity	FA Productivity [kmol/h]
1	24.61	13.33	37.95	0.98	0.90	160.1
2	20.51	11.15	31.65	0.98	0.96	171.5
3	16.77	9.32	26.09	0.98	0.97	170.3
4	16.90	9.39	26.29	0.98	0.97	170.8
5	16.30	9.05	25.36	0.98	0.95	168.0
6	16.65	9.25	25.90	0.98	0.96	169.6
7	16.65	9.26	25.91	0.98	0.95	169.7
8	16.66	9.26	25.91	0.98	0.95	169.7
9	16.36	9.09	25.45	0.98	0.95	168.2
10	16.76	9.31	26.07	0.98	0.96	170.2
11	16.47	9.15	25.62	0.98	0.95	168.8
12	16.55	9.19	25.74	0.98	0.95	169.2
13	16.39	9.11	25.50	0.98	0.95	168.4

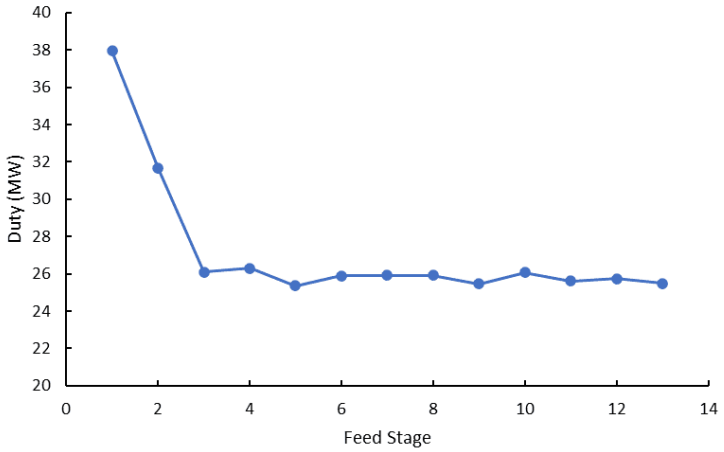

Figure E-2: Pre-fractionator feed stage correlation with total reboiler duty

Main DWC column height optimization

The optimization affects the DWC column's height, assumed to be 80% of the total stages of the non-DWC C-202 and C-203 columns. The energy-efficient best case is the sum of the non-DWC stages, 33 stages. It's crucial to note that extra stages increase both energy use and capital costs.

Table E.3: Column height optimization parameters

N	Duty Main Reboiler [MW]	Duty FA Reboiler [MW]	Total Reboiler Duty [MW]	MF Purity	Methanol Purity	FA Productivity [kmol/h]
27	21.22	9.55	30.76	0.97	0.94	167.5
28	16.70	9.51	26.22	0.97	0.94	167.1
29	16.77	9.51	26.28	0.97	0.93	165.3
30	16.57	9.48	26.04	0.97	0.93	166.2
31	16.47	9.24	25.71	0.97	0.93	166.5
32	16.41	9.12	25.53	0.97	0.94	167.1
33	16.27	9.04	25.31	0.97	0.93	166.6
35	16.24	10.49	26.74	0.97	0.94	166.6
40	16.47	10.65	27.12	0.97	0.94	167.5
45	16.48	10.65	27.13	0.97	0.94	167.5

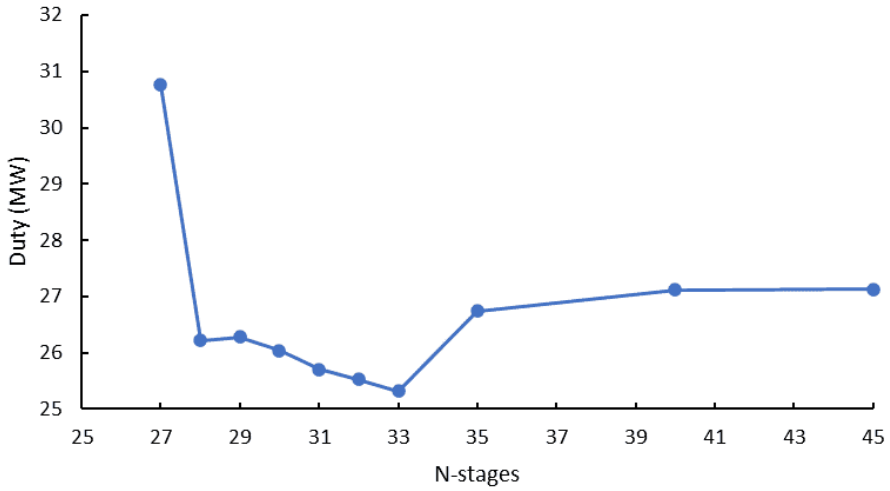

Figure E-3: Main column number of stages correlation with total reboiler duty

Main DWC column side outlet stage optimization

This optimization was also done with the stage where methanol exits as a side stream. The best case obtained from energy perspective is 19th stage.

Table E.4: Main DWC column side outlet optimization parameters

N-outlet	Duty Main Reboiler [MW]	Duty FA Reboiler [MW]	Total Reboiler Duty [MW]	MF Purity	Methanol Purity	FA rate [kmol/h]
5	18.89	10.59	29.49	0.89	0.94	166.5
6	17.71	9.90	27.61	0.92	0.93	165.4
7	16.71	9.31	26.02	0.94	0.93	163.5
8	16.99	9.47	26.46	0.95	0.94	166.1
9	16.77	9.33	26.10	0.95	0.94	166.3
10	16.55	9.21	25.75	0.96	0.94	165.7
11	17.07	9.51	26.58	0.96	0.95	169.1
12	16.82	9.36	26.18	0.97	0.95	168.5
13	16.45	9.14	25.59	0.97	0.94	167.3
15	16.49	9.16	25.66	0.98	0.95	168.3
16	16.43	9.13	25.56	0.98	0.95	168.4
17	16.59	9.22	25.81	0.98	0.95	169.4
18	16.45	9.14	25.59	0.98	0.95	168.7
19	16.30	9.05	25.35	0.98	0.95	167.9
20	16.57	9.20	25.77	0.98	0.96	169.0
21	16.59	9.21	25.80	0.98	0.97	170.8
22	16.62	9.23	25.85	0.98	0.96	169.6
23	16.65	8.91	25.56	0.98	0.93	166.7
24	17.23	9.10	26.33	0.98	0.96	168.2
25	19.64	10.63	30.28	0.98	0.91	162.9
26	50.56	27.25	77.81	0.98	0.82	152.9
27	136.04	69.98	206.03	0.99	0.64	111.4
28	158.78	81.94	240.71	0.99	0.65	113.2
29	163.27	85.48	248.75	0.99	0.71	120.8
30	144.85	75.25	220.10	0.99	0.67	118.0

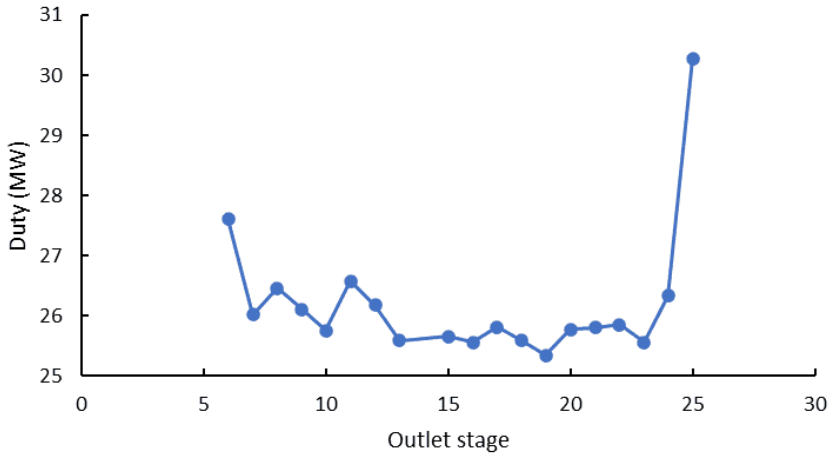

Figure E-4: Main DWC column side outlet correlation with total reboiler duty

Boil-up ratio optimization

The optimal energy consumption was observed when the boil-up ratio set to 0.9. However, with little to no energy toll productivity benefits significantly at 1 boil-up ratio.

Table E.5: Boil-up ratio optimization parameters

BUP Ratio	Duty Main Reboiler [MW]	Duty FA Reboiler [MW]	Total Reboiler Duty	MF Purity	Methanol Purity	FA rate [kmol/h]
0.4	7.36	33.83	41.19	0.97	0.93	165.48
0.5	6.82	25.11	31.93	0.97	0.94	165.58
0.6	6.56	20.29	26.85	0.97	0.96	169.83
0.7	6.40	16.99	23.39	0.97	0.97	170.42
0.8	6.48	15.12	21.59	0.97	0.98	170.43
0.9	6.15	12.94	19.09	0.97	0.95	168.38
1.0	6.66	12.79	19.44	0.97	0.97	170.57
1.1	7.20	12.59	19.79	0.97	0.97	169.62
1.2	7.67	12.27	19.94	0.97	0.95	167.86
1.3	8.33	12.31	20.65	0.97	0.95	168.53
1.4	9.14	12.55	21.70	0.97	0.96	170.01
1.5	9.57	12.24	21.81	0.97	0.95	168.41
1.6	10.30	12.36	22.66	0.98	0.96	169.39
1.7	10.97	12.39	23.36	0.98	0.96	169.54
1.8	11.61	12.39	24.00	0.98	0.95	169.79
1.9	12.22	12.35	24.57	0.98	0.96	169.52
2.0	12.54	12.02	24.56	0.98	0.93	168.12
2.1	13.38	12.23	25.61	0.98	0.95	168.96
2.2	14.01	12.23	26.24	0.98	0.94	168.21
2.3	14.72	12.29	27.01	0.98	0.95	169.46
2.4	15.45	12.36	27.81	0.98	0.95	169.94
2.5	16.04	12.32	28.36	0.98	0.95	169.77
2.6	16.68	12.31	28.98	0.98	0.95	169.82
2.7	17.28	12.28	29.57	0.98	0.95	169.63
2.8	17.92	12.28	30.20	0.98	0.95	169.65
2.9	18.33	12.12	30.46	0.98	0.95	168.69
3.0	18.99	12.14	31.13	0.98	0.95	168.73
3.1	19.66	12.16	31.82	0.98	0.95	169.06
3.2	20.64	12.38	33.03	0.98	0.96	170.27
3.3	21.09	12.26	33.35	0.98	0.95	169.71
3.4	21.73	12.26	33.99	0.98	0.95	169.73
3.5	22.36	12.26	34.61	0.98	0.95	169.73
3.6	22.98	12.25	35.24	0.98	0.95	169.73
3.7	22.79	11.79	34.59	0.98	0.94	166.89
3.8	24.26	12.25	36.51	0.98	0.96	169.73
3.9	24.48	12.03	36.51	0.98	0.95	168.42
4.0	25.21	12.08	37.29	0.98	0.95	168.85
4.1	26.02	12.17	38.19	0.98	0.95	169.46

BUP Ratio	Duty Main Reboiler [MW]	Duty FA Reboiler [MW]	Total Reboiler Duty	MF Purity	Methanol Purity	FA rate [kmol/h]
4.2	26.22	11.96	38.18	0.98	0.94	168.09
4.3	27.30	12.18	39.47	0.98	0.95	169.39
4.4	27.80	12.11	39.91	0.98	0.95	169.06
4.5	28.68	12.23	40.91	0.98	0.95	169.78
4.6	28.80	11.99	40.79	0.98	0.95	168.28
4.7	29.41	11.99	41.39	0.98	0.95	168.17
4.8	30.41	12.14	42.55	0.98	0.95	169.25
4.9	31.22	12.22	43.44	0.98	0.95	169.77
5.0	31.86	12.22	44.08	0.98	0.95	169.80

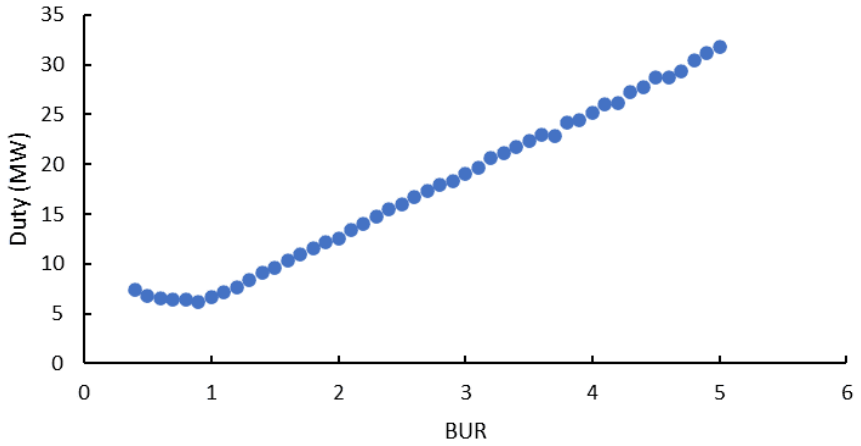

Figure E-5: Boil-up ratio optimization correlation with total reboiler duty.

During DWC and non-DWC comparison, it is crucial to have the most optimized non-DWC case as reference. Separate optimization has been done in non-DWC configuration. The summary of optimization results for both DWC and non-DWC case is presented in **Table E.6** below.

Table E.6: Final Optimization Values of the DWC design

Final Optimization Values		
	DWC	**Non-DWC**
Prefractionator		
N	13	-
N feed	9	-
Main Column		
N	33	33
Outlet	19	-
MeOH purity (molar)	96%	94%
MF purity (molar)	97%	96%
Duty (MW)	6.5	17.5
FA-Water Distillation Column		
	DWC	**Conventional**
Duty (MW)	14.6	12.2
Productivity (kg/h)	6310.1	6276.2
Productivity (kta)	50.5	50.2

F. Mass and energy balance

The mass and energy balance calculations are crucial components of process analysis. This calculation is shown as Input-Output diagram, illustrated in **Figure F-1**, which provides a comprehensive overview of material and energy flows throughout the production process.

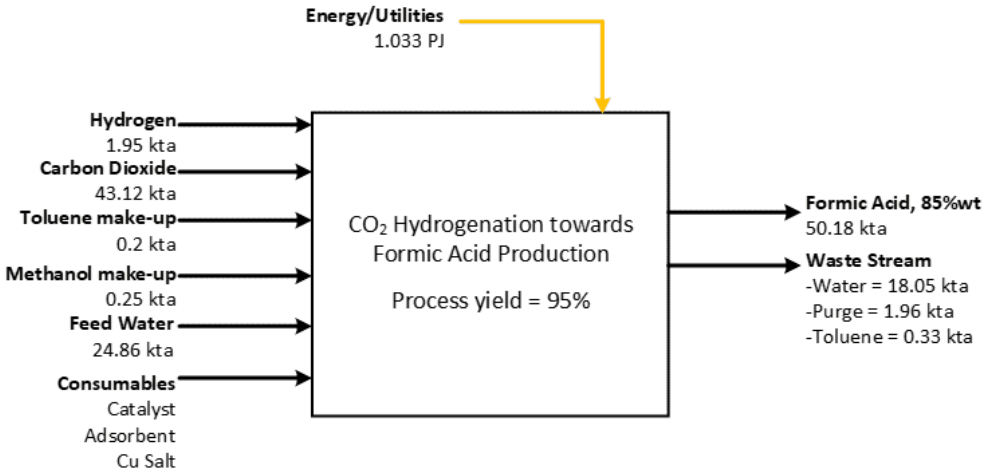

Figure F-1: Input-Output diagram of the process

G. Economic calculations

In this section the detailed information of economic calculation attributes is presented. The bare equipment cost of each unit operation and the total cost are summarized in **Table G.1**.

Table G.1: Summary of the total BEC [9]

Unit Type	Purchase cost [M€]	Base cost year
Pumps	0.42	2013
Compressors & Turbines	5.89	2013
Heat Exchangers	2.16	2013
Reactors	4.84	2013
Membrane [10]	0.35	2020
COPure™ [11]	2.16	1988
Vessels & Columns	2.63	2013
Total equipment cost	18.45	

The cost of raw materials, utilities and waste treatment is presented in **Table G.2**.

Table G.2: Summary of raw materials, utilities, and waste treatment costs

Item	Amount	Price	Purchase cost
Raw Materials	kta	€/ton	M€/yr
Hydrogen [12, 13]	1.95	2500	4.88
Carbon dioxide [14]	43.12	85	3.67
Toluene make-up [15]	0.20	900	0.18
Methanol make-up [15]	0.25	530	0.13
CO Catalyst [16]	<0.01	10^6	0.20
MF Catalyst [17]	0.35	3165	1.10
		TOTAL	10.16
Utilities	MW	€/MW	M€/yr
Electricity [18]	3.53	0.080	2.26
Natural gas [19]	7.23	0.045	2.60
Cooling Water	0.51	0.080	0.32
MP Steam [20]	15.21	28.920	4.59
LP Steam [20]	11.42	28.080	3.40
		TOTAL	13.18
Waste Treatment [21]			6.70
		TOTAL	**30.04**

CAPEX was calculated using the BEC and the relationship proposed by Peter and Timmerhaus [9]. **Table G.3** presents the detailed CAPEX calculation results.

OPEX calculation was initialized by raw materials and utilities expenses calculation (tabulated in **Table G.2**). A comprehensive overview of the overall OPEX in 2030 in the proposed plant design is provided in

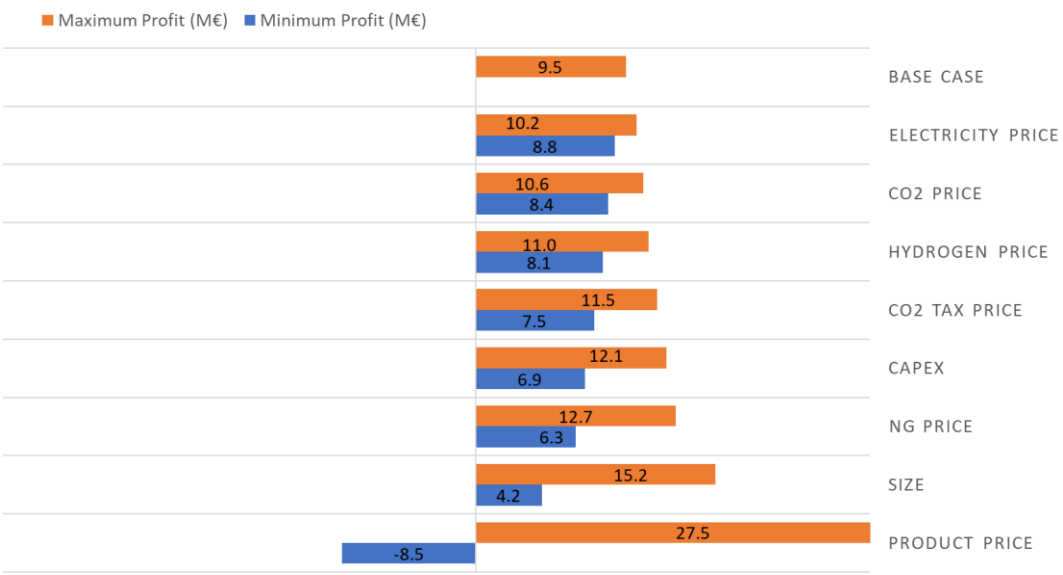

Figure G-1: Sensitivity analysis results

Table G.4.

Table G.3: Estimation of the CAPEX [9]

	% of the equipment	% of FCI	Cost [M€]
a. Direct costs			
1. Purchased equipment	100	28.7	18.45
2. Installation	35	10.1	6.46
3. Instrumentations and controls (installed)	14	4.0	2.58
4. Piping (installed)	40	11.5	7.38
5. Electrical (installed)	11	3.2	2.03
6. Buildings (including service)	18	5.2	3.32
7. Yard improvement	11	3.2	2.03
8. Service facilities (installed)	37	10.6	6.83
9. Land	6	1.7	1.11
TOTAL DIRECT PLANT COST	272	78.2	50.18
b. Indirect costs			
1. Engineering and supervision	18	5.2	3.32
2. Construction expenses	22	6.3	4.06
3. Contractor's fee	12	3.4	2.21
4. Contingency	24	6.9	4.43
TOTAL INDIRECT PLANT COST	76	21.8	14.02
FIXED CAPITAL INVESTMENT (a + b)	348	100.0	64.21
c. Working Capital	52	15.0	9.59
TOTAL CAPITAL INVESTMENT	**400**	**115.0**	**73.80**

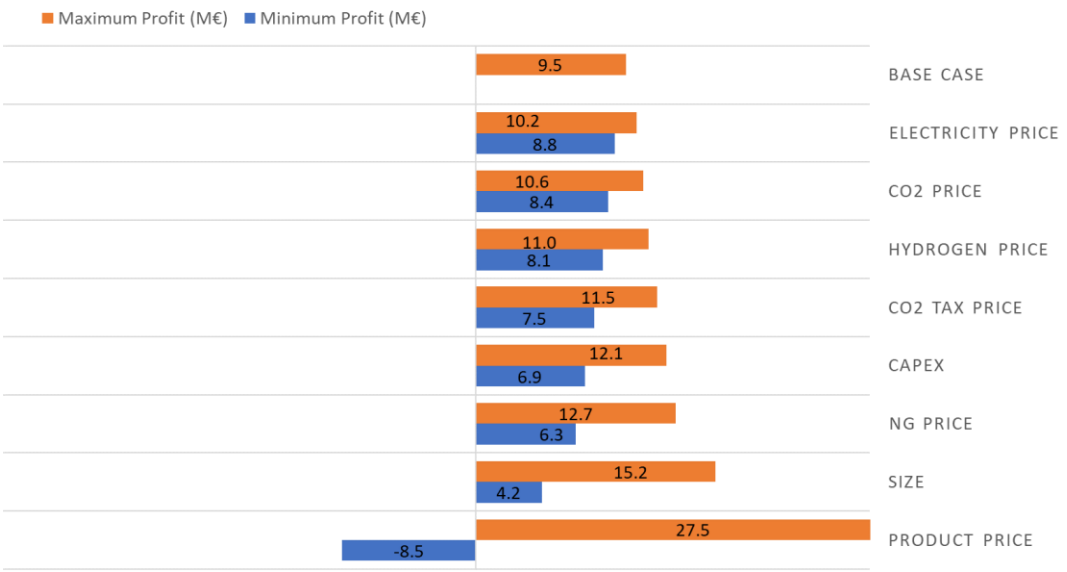

Figure G-1: Sensitivity analysis results

Table G.4: Summary of OPEX [9]

Expense	Remarks		Cost [M€/yr]
	Direct production costs		
Raw Materials			10.16
Utilities			13.18
Waste treatment			6.70
Op. labour [22]	5 operators = 3 per reaction section + 1 separation + general		1.20
Op. Supervision [23]	15% of Operating labour		0.18
Maintenance	3% of FCI		1.93
Laboratory	10% of Operating labour		0.12
Operating supplies	15% of Maintenance		0.29
		TOTAL	33.75
	Fixed Charges		
Local taxes	2% of FCI		1.28
Insurance	1% of FCI		0.64
Depreciation	4% of FCI		2.57
		TOTAL	4.49
	Plant Overhead		
Other	50% of (Op. labour + Op. supervision + Maintenance)		1.65
	General Expenses		
Administrative	20% of Op. labour		0.24
Distribution/Marketing	2% of OPEX		0.84
R&D	2% of OPEX		0.84
		TOTAL	1.91
	TOTAL OPERATING EXPENSES		**41.81**

H. Sustainability metrics

Efficient waste management is essential for sustainable chemical production, yielding to both economic benefits through reduced costs and environmental advantages in comparison with traditional pathway. In this process, sodium methoxide employed as MF synthesis catalyst is assumed to have minimal leaching risk and environmental impact. Similarly, CO separation utilizes a toluene solution containing Cu-Al chloride salt, with the assumption of no environmental leakage. However, the management of CO synthesis spent catalyst is handled separately by 3rd party and falls outside the scope of the case study. The proposal hereby also suggests utilizing wastewater from water removal processes, comprising primarily pure water, as a feed for the process, substantially reducing the need for fresh water by 73%. This initiative offers a significant opportunity to enhance sustainability by minimizing water consumption in the operation.

Gas waste arises from purging streams, which regulate the accumulation of inert substances in the system. The environmental impact can be evaluated by quantifying the $CO_{2(eq)}$ emissions from these streams. Notably, the main sources of CO_2 emissions stem from the utilization of natural gas in the fired heater in section-1 and steam generation in section-2, underscoring the necessity of developing electric alternatives to address CO_2 emissions. The analysis in **Table H.1** indicates that the process yields a carbon footprint of 1.07 kg $CO_{2(eq)}$ per kilogram of FA produced. When factoring in CO_2 neutrality, CO_2 used as feedstock was accounted, there the final CO_2 emission is greatly reduced to 0.21 kg $CO_{2(eq)}$ per kilogram of FA. CO_2 emission contributors and its portion are presented in **Figure H-1**.

Table H.1: $CO_{2(eq)}$ emission calculation for the whole process

Section	Consumption/ Production [kg/h]	Consumption/ Production [kta]		CO_2 Emission (Unit)	Total $CO_{2(eq)}$ Emission [kta]
CO Synthesis and Separation					
Natural Gas	520.3	4.16	0.05	kg CO_2/MJ	10.44
Purge					
CO	0.2	traces	2.10	GWP = $CO_{2(eq)}$	traces
CO_2	16.5	0.13	1.00	GWP = $CO_{2(eq)}$	0.13
H_2	0.5	traces	8.00	GWP = $CO_{2(eq)}$	0.03
N_2	4.3	0.03	-	GWP = $CO_{2(eq)}$	-
MF and FA Synthesis					
MF Synthesis					
LP Steam	7816.7	62.53	0.11	kgCO_2/kg Steam	7.04
Purge					
CO	119.9	0.96	2.10	GWP = $CO_{2(eq)}$	2.02
CO_2	53.7	0.43	1.00	GWP = $CO_{2(eq)}$	0.43
FA Synthesis					
LP Steam	10936.8	87.49	0.11	kgCO_2/kg Steam	9.85
MP Steam	26267.4	210.12	0.11	kgCO_2/kg Steam	23.66
TOTAL [kta]					53.61
Emission kgCO_2e/kgFA					1.07
Overall emission [kg$CO_{2(eq)}$/kgFA]					0.21

Note 1: Conversion unit 1MMBTU = 1055 MJ and Natural gas heating value of 50 MJ/kg.
Note 2: The CO_2 emission was calculated based on 90% fired-boiler efficiency.

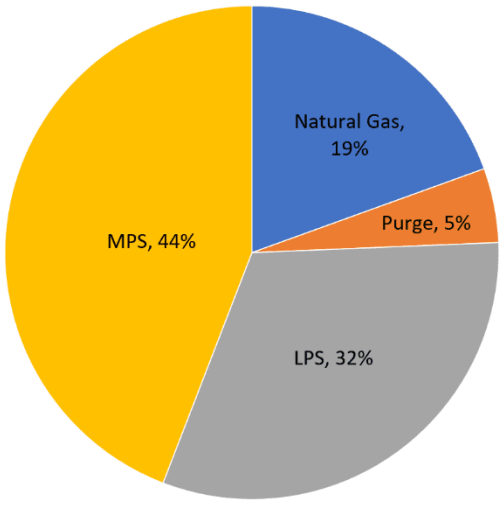

Figure H-1: Total CO_2 emission (kta) distribution in proposed green FA production

I. References

1. Tsuji, T.S., Y.; Hiaki, T.; Itoh, N., *Fluid Phase Equilib., 2005, 228-229, 499-503 Hydrogen solubility in a chemical hydrogen storage medium, aromatic hydrocarbon, cyclic hydrocarbon, and their mixture for fuel cell systems.*
2. Laugier, S.L., D.; Desteve, J.; Richon, D.; Renon, H., *Gas Processors Association Research Report, 1982, No. RR-59 Vapor-Liquid Equilibria Measurements on the Systems: N2-Toluene, N2-m-Xylene, and N2- Mesitylene.*
3. Novita, F.J., H.-Y. Lee, and M. Lee, *Self-heat recuperative dividing wall column for enhancing the energy efficiency of the reactive distillation process in the formic acid production process.* Chemical Engineering and Processing: Process Intensification, 2015. **97**: p. 144-152.
4. Liu, Z., *Methanol synthesis via methyl formate in the liquid phase*. 1988: University of Pittsburgh.
5. Abbas, Z., T. Mezher, and M.R.M. Abu-Zahra, *Evaluation of CO2 Purification Requirements and the Selection of Processes for Impurities Deep Removal from the CO2 Product Stream.* Energy Procedia, 2013. **37**: p. 2389-2396.
6. Towler, G.a.R.S., *Chapter 3 - Utilities and Energy Efficient Design, in Chemical Engineering Design* 2013, Butterworth-Heinemann: Boston.
7. Jansen, D., et al., *Hydrogen membrane reactors for CO2 capture.* Energy Procedia, 2009. **1**(1): p. 253-260.
8. Lim, Y., et al., *Techno-economic Comparison of Absorption and Adsorption Processes for Carbon Monoxide (CO) Separation from Linze-Donawitz Gas (LDG).* Korean Chemical Engineering Research, 2016. **54**: p. 320-331.
9. Peters, M.S., K.D. Timmerhaus, and R.E. West, *Plant Design and Economics for Chemical Engineers*. 2003: McGraw-Hill Education.
10. W. S. Winston Ho, K.K.S., *Membrane Handbook*. 1992: Springer New York, NY.
11. Sato, T., et al., *CHEMICAL REACTION OF CARBON MONOXIDE WITH COPPER(I)-TETRACHLOROALUMINATE(III)-AROMATIC HYDROCARBON SOLUTIONS-EQUILIBRIUM AND KINETICS.* Journal of Chemical Engineering of Japan, 1988. **21**(2): p. 192-198.
12. Editorial, I., *Green Hydrogen – the Big Unknown in the EU Power System*, in *ICIS Explore*.
13. Morgan, H., *OPINION | Why market dynamics will reduce the average price of green hydrogen to $1.50/kg by 2030.* Recharge | Latest renewable energy news, 2022.
14. IEA. *Is carbon capture too expensive? – Analysis*. IEA; Available from: https://www.iea.org/commentaries/is-carbon-capture-too-expensive.
15. ChemAnalyst. 2023 [cited 2023 1 March]; Available from: https://www.chemanalyst.com/.
16. Aesar, A., *Molybdenum Carbide, 99.5%*. 2023.
17. Arora, A. and V. Singh, *Biodiesel production from engineered sugarcane lipids under uncertain feedstock compositions: Process design and techno-economic analysis.* Applied Energy, 2020. **280**: p. 115933.
18. Eurostat. *Electricity prices for non-household consumers - bi-annual data (from 2007 onwards)*. 2023 [cited 2023 20 July]; Available from: https://ec.europa.eu/eurostat/databrowser/view/NRG_PC_205__custom_6992990/default/line?lang=en.
19. Eurostat. *Gas prices for non-household consumers - bi-annual data (from 2007 onwards)*. 2023 [cited 2023 20 July]; Available from: https://ec.europa.eu/eurostat/databrowser/view/NRG_PC_203__custom_6992966/default/line?lang=en.

20. Towler, G. and R. Sinnott, *Chapter 3 - Utilities and Energy Efficient Design*, in *Chemical Engineering Design (Second Edition)*, G. Towler and R. Sinnott, Editors. 2013, Butterworth-Heinemann: Boston. p. 103-160.
21. Netherlands, G.o. *Measures to reduce greenhouse gas emissions*. Available from: https://www.government.nl/topics/climate-change/national-measures.
22. Seider, W.D., et al., *Product and Process Design Principles: Synthesis, Analysis and Evaluation*. 2016: Wiley.
23. Peters, T., West. *Equipment Cost* [cited 2022 18 December]; Available from: https://www.mhhe.com/engcs/chemical/peters/data/.